NATIONAL AERONAUTICS AND SPACE ADMINISTRATION

Technical Report 32-1396

Primary Absolute Cavity Radiometer

J. M. Kendall, Sr.

JET PROPULSION LABORATORY
CALIFORNIA INSTITUTE OF TECHNOLOGY
PASADENA, CALIFORNIA

July 15, 1969

NATIONAL AERONAUTICS AND SPACE ADMINISTRATION

Technical Report 32-1396

Primary Absolute Cavity Radiometer

J. M. Kendall, Sr.

JET PROPULSION LABORATORY
CALIFORNIA INSTITUTE OF TECHNOLOGY
PASADENA, CALIFORNIA

July 15, 1969

Prepared Under Contract No. NAS 7-100
National Aeronautics and Space Administration

Preface

The work described in this report was performed by the Environmental Sciences Division of the Jet Propulsion Laboratory.

Acknowledgment

Without the concerted efforts of the following, this development would not have been possible.

Martin Berdahl, coinventor of the radiometer, who realized the need for the equatorial mount and electronic equipment, and provided specifications for having them made.

Clyde Sydnor, who provided analysis of the cavities and computer data reduction. R. C. Willson, for many helpful discussions on heat transfers within the radiometer.

Hunter McConnell, Jr., Lothar Kirk, and Keith Wilbert, who provided the electronic equipment and its testing.

Linus Pakulski, who provided technical assistance, particularly in fabricating the cavities and thermal resistors.

Richard Rice, Carroll Friswold, George Wagner, and Henry Cools, who provided all the design work and fabrication of the radiometer and equatorial mount.

Contents

Tables

Contents (contd)

Figures

Abstract

The newly developed primary absolute cavity radiometer (PACRAD) is based on first principles, and depends only on dimensions, arrangement of components, and electrical measurements. With this radiometer, accurate measurements of absolute solar irradiance can be made. It would also serve very well as a radiometric standard. Described and analyzed in this report, it has a windowless black cavity receptor mounted in a massive heatsink and has equal sensitivity to ultraviolet, visible, and infrared radiation. The incoming radiation is absorbed and converted into heat which flows through a metallic thermal resistor to the massive heatsink to produce a temperature difference of a fraction of a degree Kelvin. This difference is measured by a thermopile. A totally enclosed electric heater winding serves as a source of cavity heating accurately equivalent to radiation heating, and provides a built-in means of calibration. There is no temperature to control or measure. By measuring voltage and current to the heater, a known amount of equivalent power is applied to the cavity. Thermopile output is measured to give an accurate calibration of the radiometer. The design, which includes a compensating cavity and thermal resistor, minimizes all unwanted heat transfers. Their effects, all small, as disclosed by a complete thermal analysis, have been evaluated by computations and are essentially eliminated by use of correction factors, the total of which is under 0.2%, not counting the aperture correction factor. The overall *indicated* error of the radiometer is no more than 0.2%, and actually is probably less than 0.3%. The radiometer works in still air, in windy air, or in a hard vacuum. The view-limiting aperture can be made to give any acceptable angle up to a maximum of 15 deg total angle. Maximum intensity measurable is about 800 mW/cm^2. Calibration of the radiometer with the electric heater takes about 2 min. The thermopile output can be read out with a potentiometer or a strip chart recorder to provide continuous recording.

Primary Absolute Cavity Radiometer

I. Introduction

In spite of the fact that fundamental radiometry is an old science, it is still not as well developed as it might be, due no doubt to the general difficulty of making accurate quantitative measurements of radiant energy. Any development which promises improved accuracy of the radiometric standards should be reported.

This report is prepared with the belief that the newly developed PACRAD (an acronym formed from Primary Absolute Cavity RADiometer) offers some promise in this direction.

When considered as a radiometric standard, the radiometer is a receiving instrument for measuring radiation intensity throughout the ultraviolet, visible, and infrared range. This is in contrast to the standard source which generates a radiant output of accurately known intensity at a particular position with respect to the source.

The PACRAD is similar to the JPL standard total radiation absolute radiometer described in Ref. 1 in the single respect that it has a cavity receptor. The PACRAD works equally well in air or in a hard vacuum; it is view-limited while the other responds perfectly to hemispherical radiation. No part of the PACRAD differs in temperature from any other part by as much as 1°K. It has a built-in calibrating heater which provides cavity heating accurately equivalent to radiation heating.

The design that has been worked out minimizes unwanted effects, as well as lending itself to straightforward computation of the various effects which affect accuracy. These effects are compensated for, calibrated out, or eliminated by computing correction factors which make precise allowances for them.

Most of the computations described in this report to determine correction factors are approximate because of the relative complexity of the geometry of the cavity and heatsink's inside surface. More accurate computations could have been made, but it would have hardly been worth the trouble, since the nonequivalent heat transfers involved are so small. Even a 50% error made in estimation of many of the nonequivalent heat transfers would hardly affect the overall accuracy of the radiometer. In computations made in this report, 100 mW/cm^2 is taken as the comparison intensity. A summary of corrections is presented in Table 1. The calculations for obtaining the various correction factors shown in Table 1 are given in Appendix A.

The associated electronics is simple. The PACRAD, however, is not suited for determining the Stefan–Boltzmann constant, as was done with the standard

Table 1. Summary of corrections

Parameter	Reference	Correction factors
Absorptivity of cavity	Section III-B	1.00115 ±0.00050
Thermal resistance of cavity coating	Section III-C	1.00007 ±0.00005
Difference of temperature distributions in cavity cone between radiation heating and electric heating	Appendix A-II-B	1.00000 ±0.00005
Reflected radiation out of cavity cone absorbed by cavity cylinder	Appendix A-II-D	1.00029 ±0.00010
Air conduction to cavity cylinder from radiation heating of cavity aperture	Appendix A-II-G	0.99990 ±0.00005
Rereflected radiation from muffler into cavity	Appendix A-II-H	0.99991 ±0.00003
Nonequivalent heat flow from cone shield to heatsink with electric heating	Appendix A-II-I	0.99996 ±0.00003
Uncertainty in electronic measurements	Section II-E-2	1.00000 ±0.00050
Area of aperture, difference from 1 cm^2	Section II-B	0.99853 ±0.00050
Total[a]		0.99981 0.00181[a]
Radiation lost out of view-limiting aperture for acceptance angle of 5 deg	Appendix A-II-K	83.4 ±10 μW

[a]Adding up all uncertainties into a simple sum gives a total uncertainty of ±0.00181. The actual uncertainty is probably less than this amount, perhaps something like ±0.1%.

radiometer described in Ref. 1. But the accuracy of the PACRAD is equal, if not superior, to that device for the measurement of near collimated radiation such as solar radiation.

The following is a list of descriptive characteristics of the PACRAD:

(1) Absolute cavity-type radiometer suitable for application as a primary standard. Its absoluteness results from its structural arrangement and dimensions together with electrical readout equipment.

(2) Absolute accuracy better than 0.5%; resolution better than 0.05%.

(3) Constant K for absolute calibration can be checked by internal electric heater within 2 min, and as often as desired.

(4) No temperatures to measure or control.

(5) Total of all correction factors for: lack of blackness of cavity receptor, thermal gradients in cavity, and in black coating inside cavity, spurious reflections, etc., not over 0.3%. (These correction factors are individually calculable, are allowed for, and do not per se represent error.)

(6) Accuracy of measurement unaffected by any ambient air pressure from 1 atm to hard vacuum.

(7) Has no window; not affected by wind.

(8) Works perfectly in any orientation; no convection effects.

(9) Effective blackness α of cavity for collimated solar radiation: 0.999.

(10) View acceptance angle controllable.

(11) Time constant of response e^{-1} is 7 s. (A settling time of 1 min gives measurement to better than 0.1%.)

(12) Aperture area easily measured to better than 0.05%.

(13) All parts of radiometer remain at ambient temperature except cavity, which goes to about 1°C higher when irradiated with 1 solar intensity.

(14) Maximum intensity measurable: ≈6 solar intensities.

(15) Compensated for time rate of change of temperature of thermal guard and for time rate of change of ambient pressure.

The following sections of this report describe the structure of the radiometer, the associated electronic equipment, and its functioning, giving results of the effects of the various types of heat transfer occurring between the various parts of the radiometer, with derived correction factors for all heat transfers which are not equivalent to the calibrating electric heating of the cavity.

II. Description of the Radiometer

A. Physical Characteristics

Figure 1 is a photograph of the assembled radiometer, equatorial mount, and electronic box, and Fig. 2 shows a closeup of the radiometer itself. Figure 3 is a schematic showing various parts in relation to one another, giving the nomenclature used in this report. Figure 4 is a photograph of the various parts of the radiometer shown in the schematic drawing.

The radiometer consists of a view-limiting aperture, a view-limiting tube, a "muffler," and a massive thermal guard which serves as a heatsink. (The heatsink constants are given in Appendix B.)

Located in the heatsink is the cavity receptor, which is supported by a thermal resistor. The thermal resistor conducts the heat received by the cavity receptor to the heatsink. A symmetrically arranged cavity and thermal resistor serve as compensating elements. The assembly of the thermal guard and heatsink is mounted in a Dewar flask to provide an isothermal environment.

The inner housing supports the heatsink–muffler assembly in the Dewar flask. The outer housing supports the view-limiting tube and provides additional insulation.

Cavities and thermal resistors are fabricated from 5-mil sheet stock of pure silver by spinning and by silver- and soft-soldering. The cavity and thermal resistor are fabricated into one integral assembly. The receptor and compensating assemblies are soldered to the thermal joint ring, which is in intimate contact with the heatsink. The receptor cavity is internally coated with Parsons' black lacquer.

A thermopile measures the temperature difference across the thermal resistors. The thermopile output electromotive force (emf) is a measure of the radiation intensity being measured.

The cavity effect enhances the absorptivity α and emissivity ϵ of the cavity aperture over that of a simple flat surface. It also decreases the disturbing effect of the thermal resistance of the black coating used inside the cavity as well as making the receptor less sensitive to the spectral quality of the incoming radiation.

For a 5-deg acceptance angle, the radiometer must be aimed at the source within 0.4 deg. The aiming sights provided on the radiometer make it easy to achieve this accuracy. Once the aim is established, the equatorial mount accurately maintains the aim.

The purpose served by the view-limiting tube and muffler, each with its diaphragm radiation stops, is to provide an acceptance angle of 5–15 deg and to provide protection from wind for the cavity receptor. The muffler is in perfect thermal contact with the thermal guard and acquires the same temperature to within a few thousandths of a degree Kelvin. A pinhole sighting arrangement is used for aiming the radiometer at the sun with an accuracy of about 0.1 deg.

Since it is difficult to make a spaced winding for the heater on an external conical surface, several designs were made with the heater winding on the cylindrical portion of the cavity. These designs relied on the excellent thermal conducting properties of the silver cavity shell to provide the necessary isothermality. They are shown in Figs. 5a, b, and c. Analysis of each showed that the correction factors were relatively large and difficult to estimate accurately. After a bit of effort, however, a practical procedure was worked out for putting the heater winding on the conical portion of the cavity, which, during calibration, provides almost exact equivalence of electric heating to radiation heating of the cavity. This cavity arrangement, shown in Fig. 5d, was incorporated in the final design. As can be seen, the heater is completely enclosed by the cone shield toward the back, and by the cavity toward the front. Of the heat electrically generated, 99% flows from the heater winding to and through the conical portion of the cavity cone, and 1% flows by air conduction to and through the cone shield.

The equipment shown in Fig. 1 can be powered from the 115 V ac line, or from portable batteries when the equipment is to be used in remote locations.

The radiometer shown in Fig. 2 weighs almost 14 lb because of the heavy copper heatsink and copper and brass housings. A second radiometer has been built in which magnesium has been substituted for almost all the metal parts. Because of this substitution, the overall weight has been reduced to 2.2 lb, with no degradation of performance.

Appendix B gives some heatsink constants of the radiometer.

B. Cavity Aperture

The copper cavity aperture is shown in general relation to the rest of the radiometer in Fig. 3, and in detail in Fig. 6.

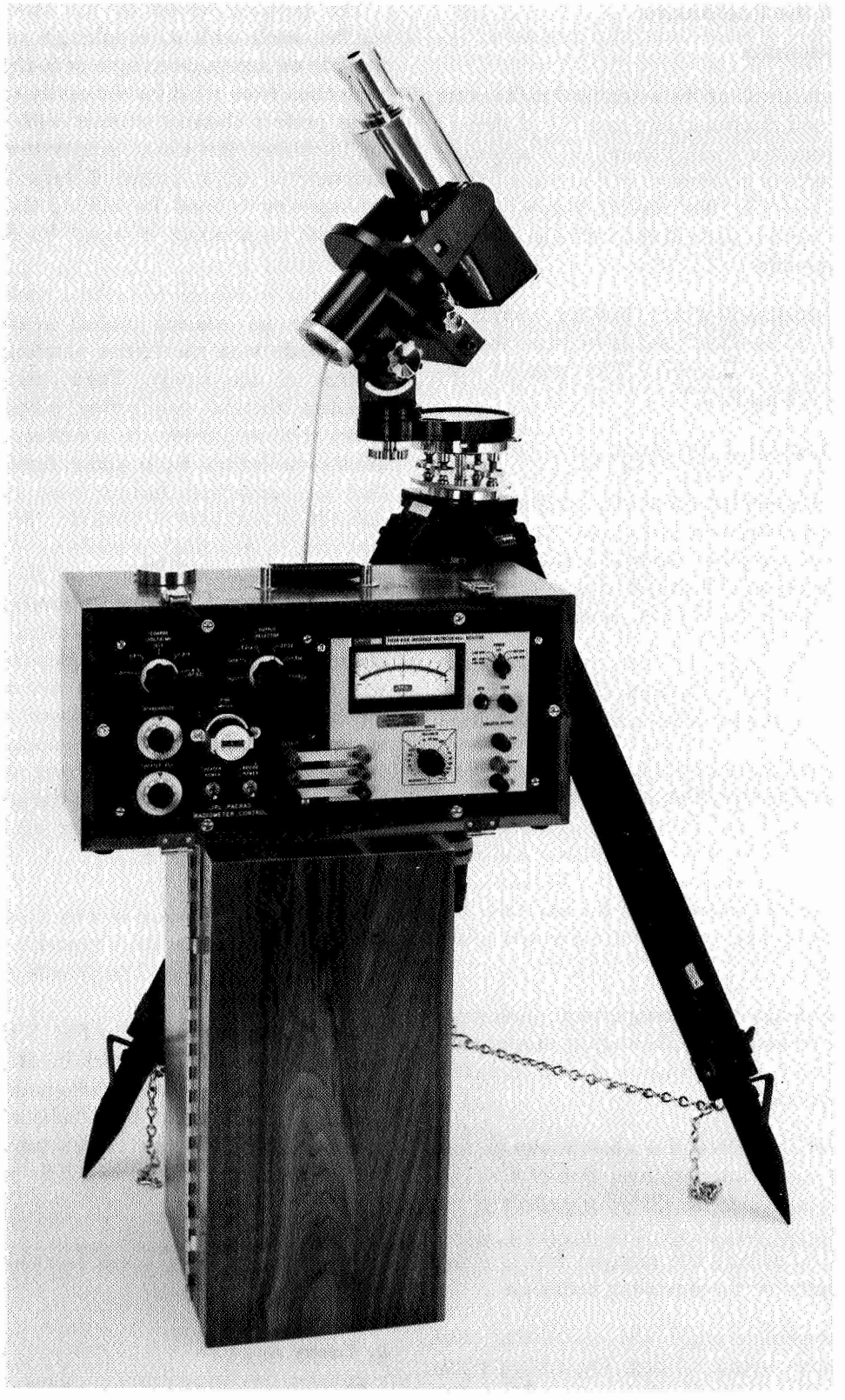

Fig. 1. Photo of overall equipment, radiometer, equatorial mount, and electronic box

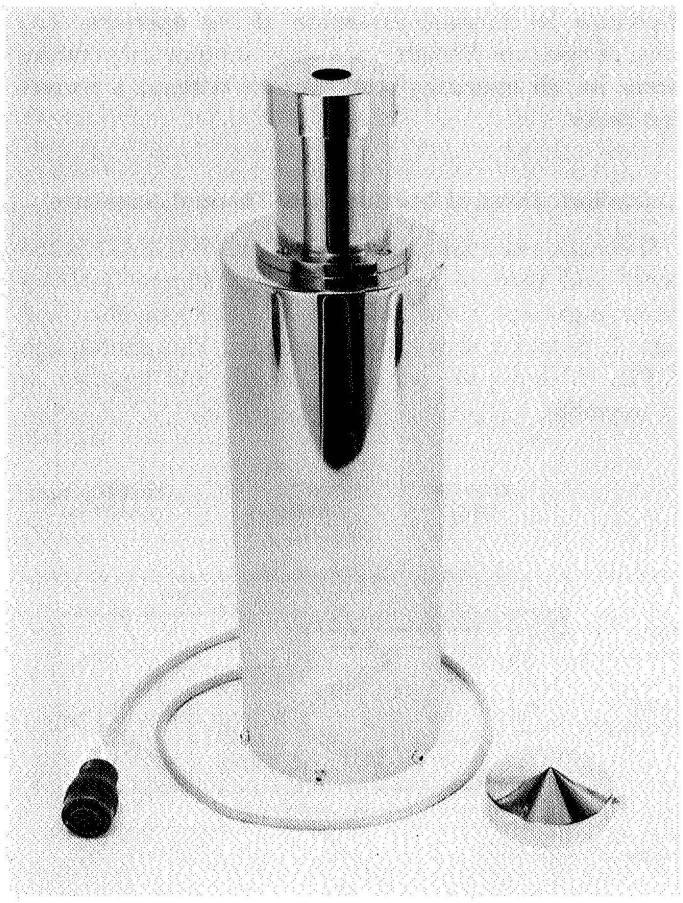

Fig. 2. Photo of assembled radiometer

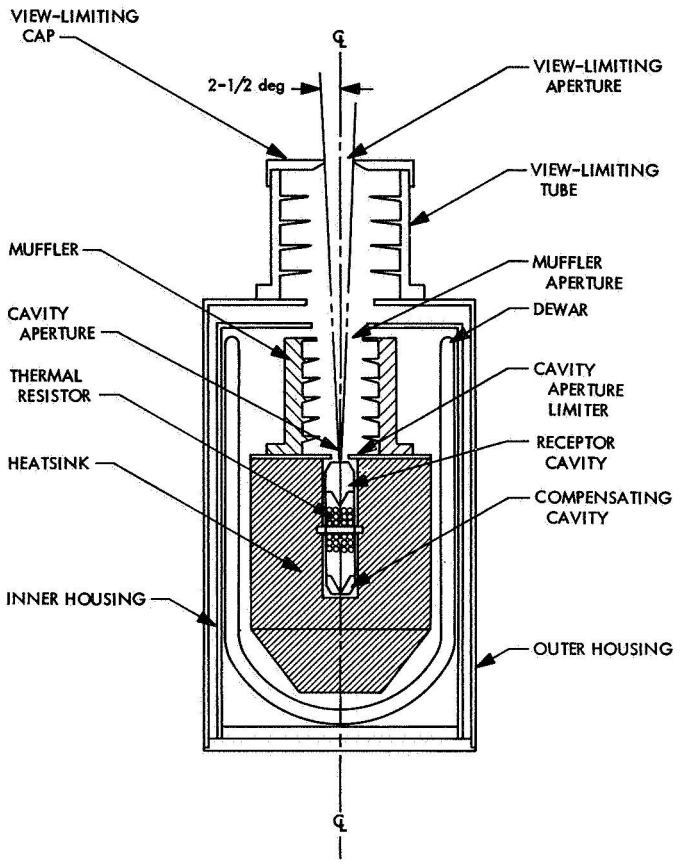

Fig. 3. Schematic of radiometer

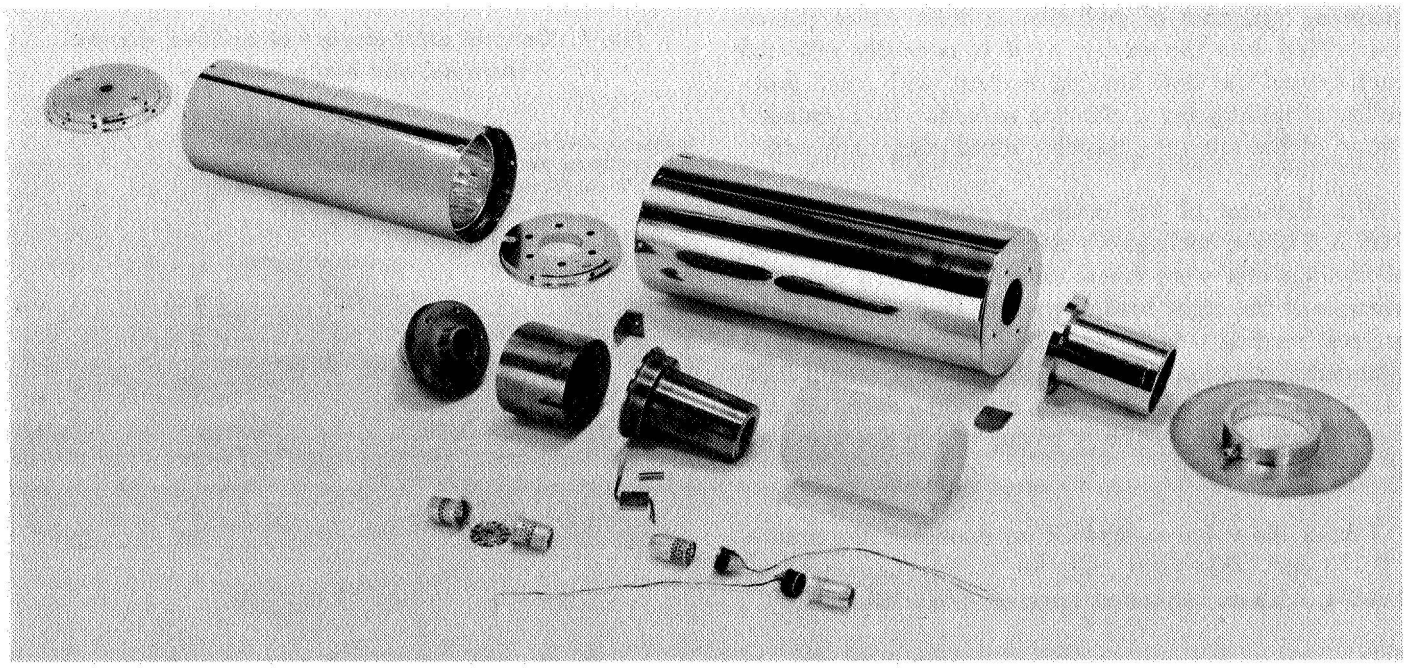

Fig. 4. Exploded view of electronic parts

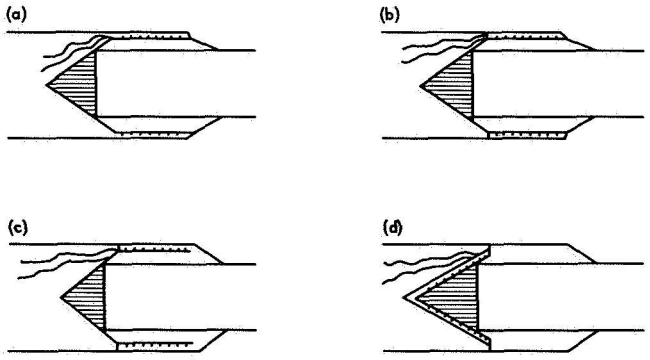

Fig. 5. Four cavity arrangements investigated

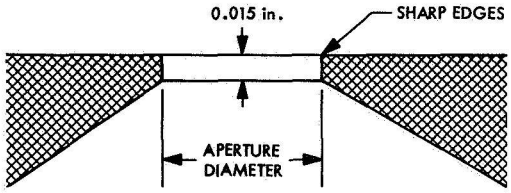

Fig. 6. Cavity aperture

The area of the cavity aperture is one of the most critical quantities bearing on the overall accuracy of the radiometer; therefore, it is necessary to obtain the most precise determination of the area possible. For the sake of convenience, the area was made as near 1 cm^2 as feasible. Considerable effort was made to give a sharp edge to the entering corner of the aperture hole. An incoming quantum of radiation is then either passed unmodified into the cavity, or it is normally reflected back toward the view-limiting element, with small probability of undergoing a glancing reflection by a rounded corner of the aperture, thereby introducing uncertainty.

The diameter of the cavity aperture was measured with a Unitron toolmaker's microscope. Eight readings of the diameter were taken, one for each 22½ deg. The average of the eight readings was 0.44457 in., with the greatest reading 0.44460 and the smallest 0.44455 in. A systematic variation over the eight readings would indicate lack of roundness, but only a random variation was seen; hence, the aperture is round within the accuracy of the measurements.

Taking the value as 0.44457 in. diameter, the area is 1.00150 cm^2. This value calls for a correction factor of 0.99854, with an estimated error of <0.00050.

Since the radiometer is always operated at close to room temperature, there is no necessity of making any allowance for thermal expansion of the aperture. The value of aperture diameter measured at room temperature serves for all operating temperatures without a correction factor.

C. Cavities, Thermal Resistors, and Thermal Junctions

The most essential component of the PACRAD is the cavity and thermal resistor assembly. Figure 3 shows the arrangement in the radiometer of this assembly, and Figs. 7, 8, and 9 show specific details. The photograph of Fig. 10 shows the parts individually and together as an assembly.

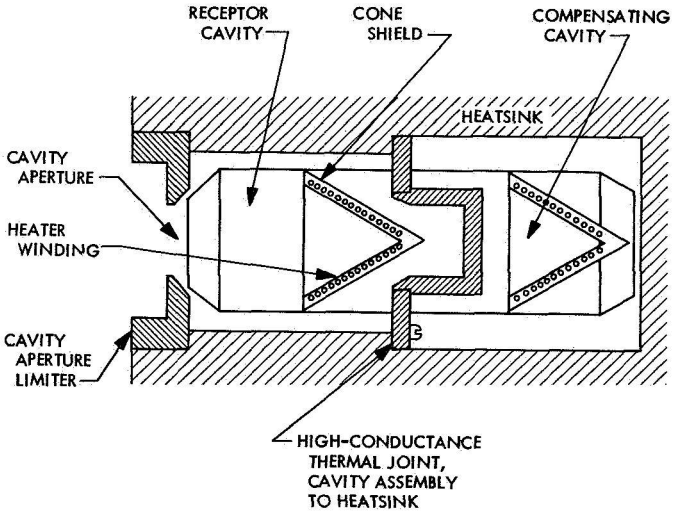

Fig. 7. General arrangement of cavities, thermal resistors, and heater winding

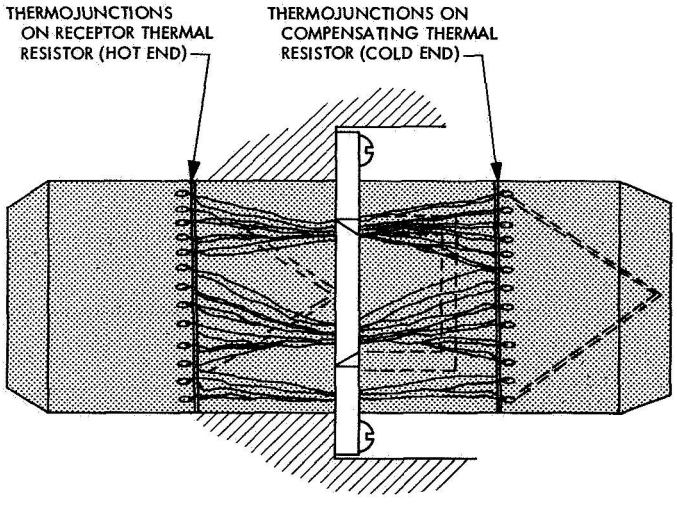

Fig. 8. Arrangement of thermocouples on receptor and compensating cavities

1. Physical description. There are two cavities and two thermal resistors which are essentially identical. The thermal resistors are joined together back to back, and the assembly is joined to the heatsink by means of a high-conductance thermal joint, which is a ring-shaped piece of copper. The opposite ends of the thermal resistors are joined to their respective cavities as shown. Figure 7 shows how the heater winding is enclosed by the conical portion of the cavity and the cone shield. All joints are either silver- or soft-soldered, so that the thermal resistance of each joint is zero. By being totally enclosed, the heater winding cannot lose heat: All heat generated by the electric heater winding must go into either the silver cavity cone or the cone shield—none can escape.

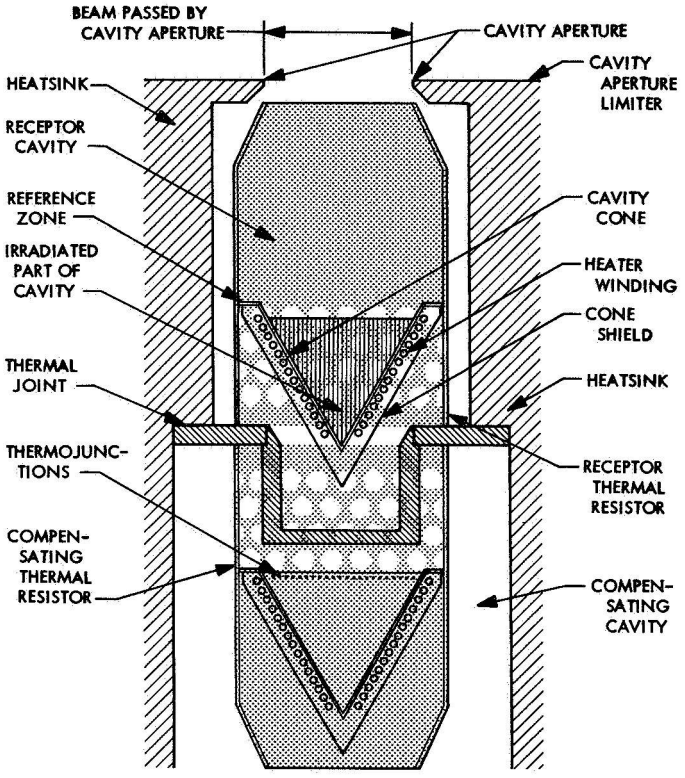

Fig. 9. Arrangement of receptor and compensating cavities in heatsink

The thermal resistors are silver cylindrical shells 5 mils (0.127 mm) in thickness. Four rows of holes are drilled in the silver near the junction with the high-conductance attachment. These holes increase the thermal resistance of the cylinder to the required value.

As shown in Fig. 8, the 16-pair thermopile generates an emf proportional to the difference of temperature ΔT between the ends of the thermal resistors.

When neither radiation heating nor electric heating is applied to the cavity receptor, the temperature drop across the thermal resistor goes to zero and the thermopile output likewise goes to zero. When either type of heating (say, equivalent to 100 mW/cm^2) is applied to the cavity, it warms it to a little less than 1°K above the temperature of the heatsink, and the thermopile generates an output of almost 1 mV.

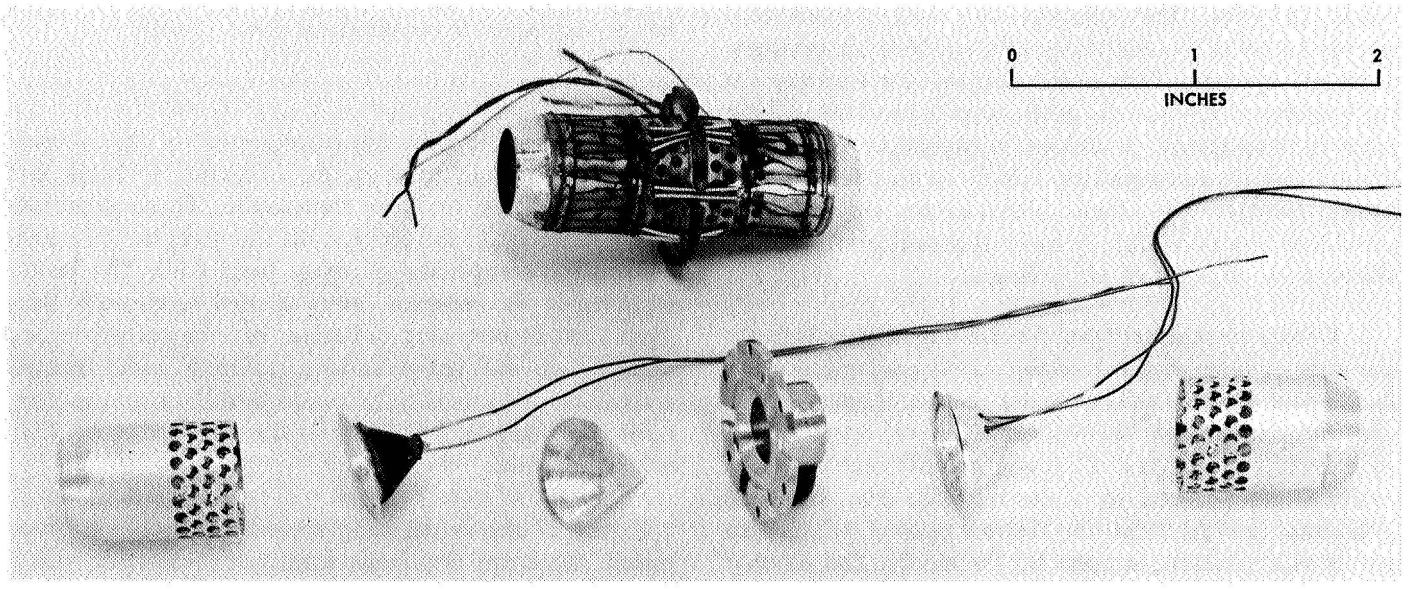

Fig. 10. Photo of cavity assembly and exploded view of cavity parts

When the cavity receptor receives heat, the heat flows through the receptor thermal resistor to the high-conductance joint. At this time, no heat flows in the compensating thermal resistor, and the compensating cavity remains at the heatsink temperature.

2. *Temperature compensation.* When the heatsink is in process of changing temperature ($dT/dt \neq 0$), the heat capacity of each of the cavities prevents them from following the heatsink temperature change rapidly; that is, their temperature lags behind the heatsink temperature. Since the heat capacities of the cavities are equal, and the thermal resistors likewise are equal, the cavity temperatures remain equal to each other during the time the cavities are changing temperature, thereby providing compensation for the rate of heatsink temperature increase.

Since the heatsink is well insulated by the Dewar flask, it will change temperature only when it absorbs or loses heat through the view-limiting aperture, or whenever there is electric heating of the receptor cavity.

The area of the 5-deg view-limiting aperture is about twice the area of the cavity aperture; thus, if the intensity of the incoming radiation is 100 mW/cm^2, about 200 mW is being absorbed by the heatsink—half through the cavity, and half through the cavity aperture limiter. As a result of this absorption, the heatsink temperature slowly increases.

Without the compensating cavity and resistor arrangement, the heatsink rate of change of temperature would cause an error. The compensating arrangement also proves to be of benefit when the ambient air pressure suddenly changes. This could happen, for example, in an aircraft cabin when the radiometer is used for making solar measurements. A sudden compression of air increases the air temperature, which—with the compensating arrangement—affects both cavities equally, thus providing compensation. Hence, the radiometer is not affected by changes of air pressure.

3. *Cavity arrangement and functioning.* Figure 9 shows the arrangement of the receptor cavity and its location inside the heatsink. The cavity has a short tapered section (immediately behind the cavity aperture), a cylindrical portion, and a closing conical rear end (the cavity cone) covered by a cone shield. The extended cylindrical portion forms the thermal resistor, which also serves as a mounting support for the cavity. The thermal resistor is thermally attached to the heatsink by the low-resistance thermal joint.

Shown in the sketch (Fig. 9) is the incoming beam of radiation passed by the cavity aperture; also shown is the region in the conical end which the beam irradiates. The outside surface of the irradiated portion of the cone is covered by the electric heater winding which, during calibration with zero irradiance, provides heating almost identically equivalent to that produced by absorption of the incoming radiation. There is a temperature drop of approximately 0.1°K (as determined by measurement) between the heating wire and the silver in the cone, which produces some excess radiation, and which is either effectively absorbed by the cone shield or reflected back to the winding. The heat absorbed by the cone shield is conducted to the "reference zone" shown in Fig. 9. With the heater winding so disposed and shielded, the heating is accurately equivalent to radiation heating. In other words, heat produced by the heater winding affects the thermal resistor exactly the same way as heat produced by absorption of incoming radiation. All the heat, either from radiation or from electric heating, finds its way to the reference zone, and from there sets up a temperature distribution in the cavity and thermal resistor. Even though the heater winding is 0.1°K hotter than the silver in the cone, the silver is at almost the same temperature as if there were no 0.1°K drop. All of the heat generated in the winding is forced through the thermal resistor in the same manner as radiation-generated heat.

The net result of generating heat by electric heating in the same place where heat is produced by absorption of radiation is that electric heating is accurately equivalent to the radiation heating, with the result that no correction factor is required for these effects.

D. Circuit

Figures 7 and 8 show the arrangement of the receptor and compensating cavities, their thermal resistors and heater windings, and the thermopile. Thermojunctions of the thermopile are located on the receptor (hot end) and on the compensating cavity (cold end). The heater winding on the receptor cavity is used to generate heat equivalent to incoming radiation, but the corresponding winding on the compensating cavity is never heated electrically; it is used only to add into the compensating cavity the same heat capacity as does the heater winding on the receptor.

Figure 11 shows the basic measuring circuit; as illustrated, there are two leads from the thermopile which carry thermopile output emf to be measured. As Fig. 12 shows, there are four leads from the receptor heater

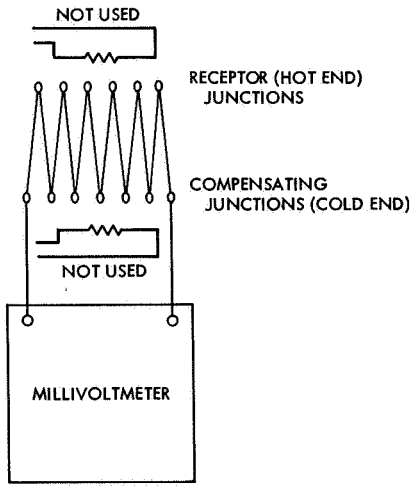

Fig. 11. Simplest possible circuit diagram

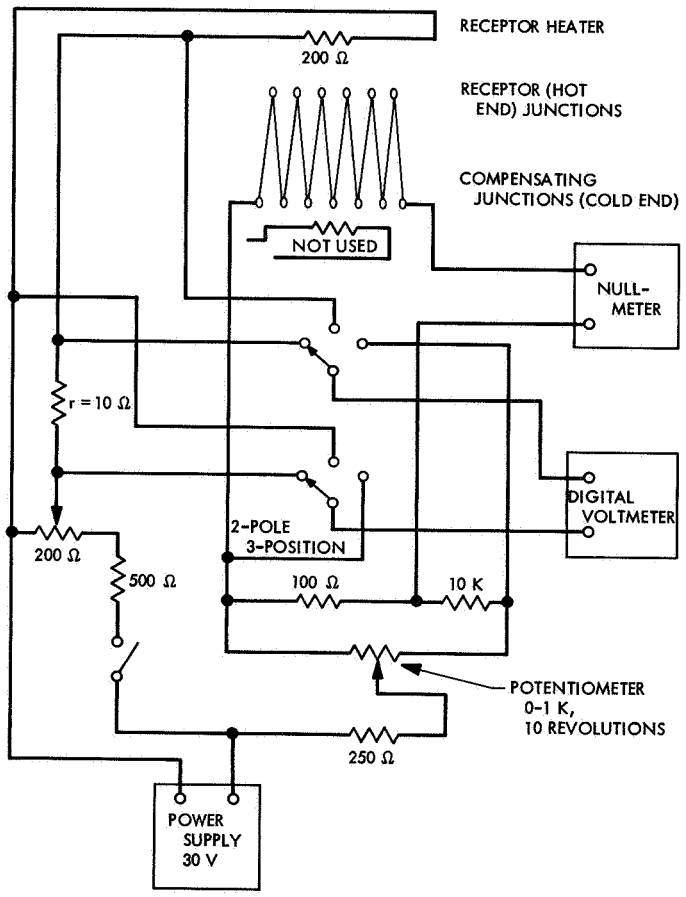

Fig. 12. Schematic of circuit with digital voltmeter readout

winding: two for carrying current to the heater and two for accurately measuring the voltage across the heater winding. A 2-pole, 3-position switch permits a digital voltmeter to be connected to measure the output emf of the thermopile as well as heater current and voltage. With the cap on the radiometer, by measuring both voltage and current applied to the receptor heater, the heater power can be calculated. With the thermopile output response to heating power, and with the overall correction factors for the various thermal effects, the radiometer calibration constant can be obtained.

In actual practice, calculating the calibration constant requires about 2 min. Similarly, data reduction requires 2 min (using a slide rule). After the calibration constant has been determined, an accurate radiation intensity measurement can be made in 1 min.

E. Measurements

1. Data reduction. The data reduction for radiometric measurements consists of multiplying the calibration constant K with the thermopile output emf obtained from the measurement, plus the amount of radiant power lost through the view-limiting aperture (0.0834 mW).

The relationship of the following quantities is shown in Fig. 13.

$\frac{E_r}{r}$ = current I through resistance R, in amperes

$E_p - \frac{E_r}{r}\ell$ = potential E across R, in volts

$\left(E_p - \frac{E_r}{r}\ell\right)\frac{E_r}{r}$ = electric heating power EI

$\frac{Cf\,EI}{v_{cal}}$ = calibration factor K

Cf = correction factor for thermal effects and for aperture area

W_{in} = input power, in watts per square centimeter (W/cm²)

W_L = power lost through view-limiting aperture during a measurement, in W/cm²

v = thermopile output voltage obtained from radiometric measurement

v_{cal} = thermopile output voltage obtained from digital voltmeter readout (used for calibration)

ℓ = internal lead resistance

The working equation is

$$W_{in} = \frac{EI\,Cf}{v_{cal}}\,v + W_L \qquad (1)$$

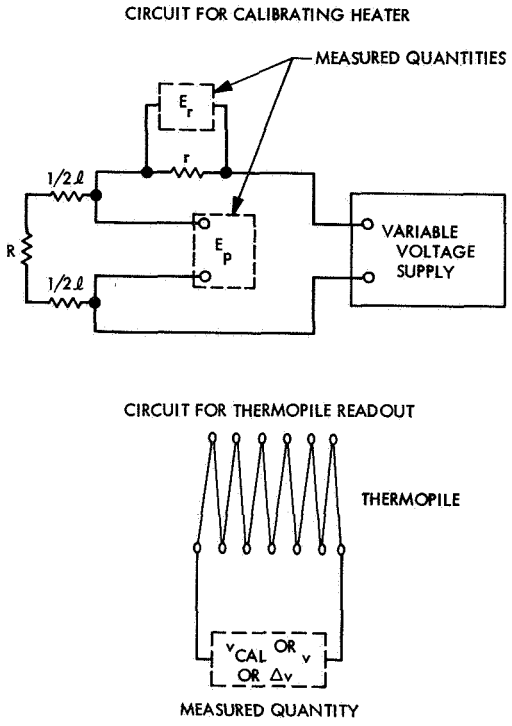

Fig. 13. Simplified schematic of electric circuit

A small offset emf can be produced by several different causes, such as the view-limiting tube differing in temperature from that of the cavity, or by parasitic thermal emf produced anywhere in the circuit, or by an offset zero reading of the nullmeter. Any error resulting from such offset emf can essentially be eliminated by making a radiometer calibration under the conditions producing the offset. The offset is than calibrated out. Appendix C considers this situation in detail.

2. Accuracy of electronic measurements. Thanks to the generally advanced state of electronic measurements, no significant loss of accuracy need occur in the use of the PACRAD for measurements of irradiance.

Required is an accurately known value (to within 0.01%) of the fixed resistor r shown in Fig. 13. Accurately measured values of the three voltages E_p, E_r, and v or v_{cal} are also required. These voltages are measured with a precision potentiometer such as that shown in Fig. 1, or by a digital voltmeter (Hewlett-Packard 3460A, or equivalent) which has 5-place accuracy. E_p and E_r are directly measured, and v or v_{cal} are also measured by the digital voltmeter (with the aid of a Lindeck circuit and nullmeter sensitive to 0.1 μV) or with the high-quality potentiometer.

All members of the expression for W_{in} (denoting W/cm^2), which depend on electronic measurements (the thermal correction factors and W_L are calculated), must be accurate to within 0.05%.

III. Thermal Characteristics

A. Heat Transfers—Wanted and Unwanted

When the radiometer receives neither radiation nor electric heating, it comes to an overall isothermal state ($\pm$0.001°K) within about 1 min. The thermopile then generates zero emf.

With incoming radiation, heat is produced in the cavity cone. While most of this heat flows through the metallic thermal resistor to the heatsink, some of it bypasses the thermal resistor and flows to the heatsink through various paths.

By considering the heat leaving or entering the cavity over each part of its inner and outer surfaces, it is possible to recognize the various heat transfers. Given in decreasing order of magnitude, the means of these heat flows are: metallic conduction, air conduction, and radiative transfer. Heat transfer by convection has been found to be insignificant. If the radiometer is operated in a vacuum, heat transfer by air conduction is, of course, nonexistent. A detailed analysis of the thermal coupling is provided in Appendix B-I.

Figure 14 is a schematic overall representation of the radiometer heat transfers. The heavy lines and arrows show the path of the primary flux from the incoming radiation, through the cavity coating, the cavity cone, past the reference zone, through the thermal resistor, and into the heatsink. Mostly unwanted (but unavoidable) are the small numerous secondary heat transfers which are due to air conduction and radiative heat exchanges. These heat transfers are indicated in the diagram by light lines and arrows.

Radiative heat exchanges occur when temperature differences exist in radiometer components that lie in opposition to one another. An analysis of the effects of such transfers is included in Appendix A. (The equations shown in the appendix were used as sources for a number of "correction" factors.)

A complete thermal analysis of the radiometer was made in which every recognizable type of heat transfer

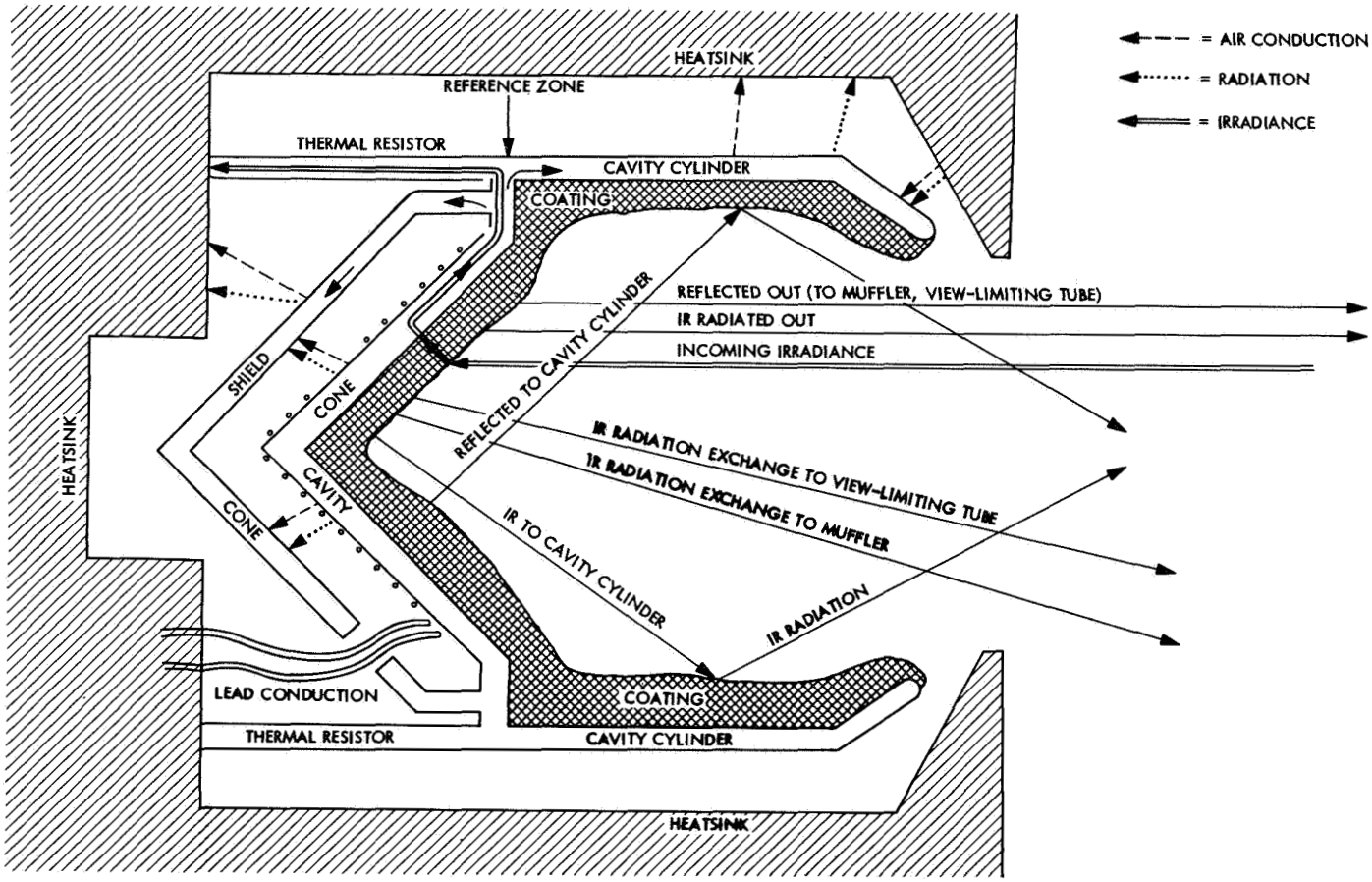

Fig. 14. The pattern of heat transfers

was investigated. Where appropriate, correction factors were deduced to prevent loss of accuracy by making allowance for all such nonequivalent heat transfers.

The construction and conditions of operation are such that the maximum temperature difference produced by the total of all heat flows which occur in the radiometer is always less than 1°K. This difference occurs between the cavity and heatsink, either for one solar intensity irradiance or for the equivalent electric heating. The higher the value of the thermal resistor, the greater the difference in temperature between the cavity and the heatsink. The particular value chosen represents a compromise. A high value of thermal resistance gives high sensitivity to the radiometer with increased output voltage from the thermopile, but it also increases the time constant and length of time one must wait for the output emf to stabilize.

In estimating correction factors for the various unwanted heat transfers, it is necessary to distinguish between equivalent and nonequivalent heat transfers. The equivalence relates to the degree to which electric heating of the cavity duplicates heating produced by incoming radiation. Incoming radiation produces one pattern of heat transfers; electric heating produces a slightly different pattern. It is the purpose of the following subsections to identify all types of heat transfer and to determine how each of those due to incoming radiation differ from corresponding heat transfers produced by electric heating. Such differences are nonequivalent and require the application of correction factors. Since the nonequivalent heat transfers are very small compared to the equivalent heat transfers, and are *linear* in nature, the superposition theorem holds. This means that small effects can be legitimately added or subtracted to obtain a correct overall result.

Electric heating sets up a temperature distribution which is very nearly the same as that set up by radiation coming into the cavity. This distribution is *nonequivalent* to radiative heating to the extent that its effect on the thermopile differs from that produced by incoming radiation. Deviations from exact equivalence are of great

importance, and occur, for example, under these conditions:

(1) A difference of temperature distributions exists between radiative heating and electric heating.

(2) A part of the incoming radiation is reflected out (or emitted, as with infrared radiation) through the aperture.

(3) A thermal resistance in the coating causes a temperature drop in the coating.

(4) Infrared radiation is emitted into space due to cavity temperature.

Considerable effort was expended to arrive at a radiometer design which has the smallest possible number of undesirable types of heat flow and with the smallest magnitudes. None of the individual disturbing heat flows is as large as 0.2%, and altogether (disregarding sign) they total less than 0.3%. This figure does not represent error; correction factors have been deduced which should make the error much smaller than 0.3%.

Radiative heat transfer frequently requires the use of *view factors*, which have been used several times in computing unwanted heat transfers. A brief discussion of view factors sufficient for the needs of this report is given in Appendix A.

B. Effective Absorptivity of Cavity

The effective absorptivity to incoming radiation of the irradiated cavity cone was calculated for incoming collimated radiation by using a modified form of Sparrow and Jonsson's method for cones (Ref. 2). The actual computation was made using an IBM 1620 computer.

Figure 9 shows the cavity, its essential proportions, and the portion of the cavity cone illuminated from the incoming collimated radiation. The computation was made for a coating of Parsons' black lacquer with an absorptivity of 0.98 (see, for example, Ref. 3), and is for the illuminated conical portion only. The beam entering the conical portion is 1 cm² in area. When the surface absorptivity is 0.98, the effective absorptivity of this portion of the cavity was computed to be $\alpha_{eff} = 0.98884$ for collimated irradiance.

The cavity as a whole, however, has an absorptivity considerably greater than the absorptivity of the conical portion alone. This comes about because only a portion of the radiation reflected by the conical portion escapes through the cavity aperture. That which does not escape is almost completely absorbed by the blackened walls of the cavity cylinder after several internal reflections. The view factor (see Appendix A) for the radiation escaping through the cavity aperture from the illuminated portion of the cavity cone is $F_{1-2} = 0.10$.

For collimated radiation the reflectance of the conical portion is $1 - 0.988838 = 0.0111$. The portion of radiation escaping through the cavity aperture is $0.0111 \times 0.010 = 0.00111$.

Of the radiation reflected from the cavity cone, 90% is absorbed by the cavity cylinder. If allowance is made for the radiation reflected the second time in the cavity cylinder, calculation shows that the radiation escaping is about 0.00004 more, making a total reflected radiation out of the aperture of $0.00111 + 0.00004 = 0.00115$, calling for a correction factor Cf of 1.00115. The overall absorptivity of the cavity is $1 - 0.00115 = 0.99885$.

Figure 15 shows a plot of effective absorptivity of both the conical portion of the cavity and of the overall cavity as a function of the absorptivity of the coating alone.

If $\alpha_{coat} = 0.985$, then $\alpha_{cav} = 0.99916$, and the correction factor is 1.00084. Thus, an increase of 0.5% in α_{coat} causes an increase of 0.0021 in the overall absorptivity.

C. Thermal Resistance of Coating

Parsons' black lacquer, which is used inside the cavity to make the internal surface optically as black as possible, is not a very good thermal conductor compared to metals.

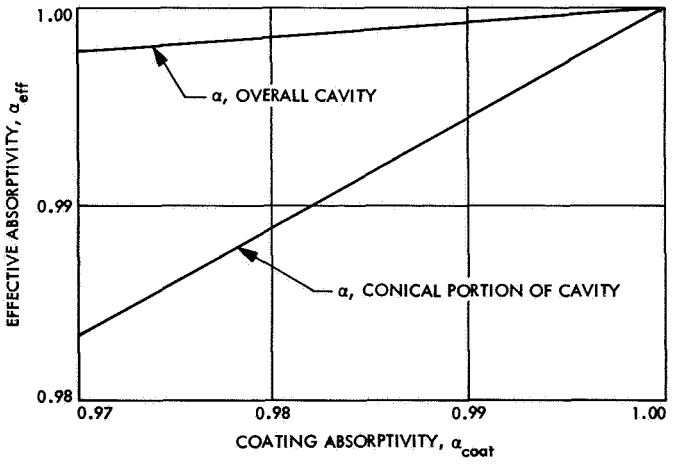

Fig. 15. Effective absorptivity of conical portion of cavity and of overall cavity as a function of absorptivity of coating alone for collimated incoming radiation

When radiation strikes the surface of the coating, the radiation is absorbed and tends to heat the surface of the coating. Most of the heat thus produced is conducted through the coating into the silver substrate of the cavity cone. Due to the thermal resistance of the coating, the temperature of the outermost layer is hotter than the layer in contact with the silver substrate. Hence, the top layer is radiating a little more energy away than it would if the thermal conductivity of the coating had no resistance. This effect requires a correction factor.

The thermal resistance of Parsons' black lacquer is not too well determined at present. One published value, 2.5°C/W/cm², is that of Blevins and Brown (Ref. 4) and is for a coat of "ordinary thickness."

The actual value may possibly be lower than that given. If the value is lower, the temperature drop through the coating is of course decreased, which is quite satisfactory. However, assuming the value is as high as the published figure, the performance of the radiometer is still not degraded.

For a *flat* coated surface out in the open, incoming radiation of 100-mW/cm² intensity would cause a temperature drop of 0.25°C. In the cavity, the surface is not flat, and the rays of collimated radiation do not strike the surface normally. The half-angle of the cone of the cavity is 30 deg so that the heat flux per square centimeter through the coating is decreased by sin 30 deg = 0.500. The drop then is $0.500 \times 0.25 = 0.125$°K.

The temperature of the outermost layer of the coating then has an excess temperature of 0.125°K which causes it to radiate a little more than it would if there were no drop. The surface of the coating is at 300.125°K, whereas if there were no thermal resistance in the coating it would be at 300.00°K. Radiation taking place from a surface at 300°K is in the infrared (about $\lambda = 9$ μm). The emissivity of the coating at this temperature is about 0.945. The amount of the excess radiation from the coating surface is

$$\alpha dW = \frac{4A\,\epsilon\sigma T^4\,dT}{T} = \frac{4 \times 1 \times 0.945 \times 0.0460 \times 0.125}{300}$$

$$= 0.0000730\text{ W } (0.0730\text{ mW})$$

Of this amount, only 10% (0.0073 mW) escapes through the cavity aperture due to the view factor of the illuminated portion of the cone to the aperture. The ratio of the loss through the aperture compared to the incoming intensity is 0.0073/100 mW = 0.000073, or 0.0073% loss. The corresponding correction factor *Cf* is 1.000073. The amount of heat energy absorbed by the cavity cylinder to heat it is $0.90 \times 0.000073 = 0.000066$ W (0.066 mW).

IV. Time Responses

The radiometer time response is such that about 1 min is required for the thermopile output emf to become completely stabilized after a sudden change of input irradiance. The so-called time constant ($1/e$) is about 7 s. Eight such time constants requiring about 1 min give a stabilization to within less than 0.1%.

This time constant is determined principally by the product of thermal mass of the cavity and the thermal resistance of the thermal resistor.

An additional time-response effect is due to the mass and thermal resistance of the muffler, which may be characterized as a bar heated at one end. The time response of this affects the amount of thermal radiation from the muffler entering the cavity.

The third time response which has been recognized is of little more than academic interest because of its small effect. This time response is due to the entrapped air in the radiometer which is between the cavity and the heatsink. Since air has thermal mass and thermal conductivity, it requires a finite time for a heat flow via the air to become fully established. As shown in this report, this stabilization time is short enough to be neglected.

Appendix D considers the first two of the above-mentioned time responses.

V. Concluding Remarks

Three models of PACRAD have been built. PACRADs I and II are virtually identical; both have heavy copper heatsinks. Analysis in this report is for PACRAD II. PACRAD III has a magnesium heatsink and no Dewar flask. It weighs 2.16 lb. Tests have shown that all three models agree with one another within 0.15%.

Several tests have been made in which PACRADs were compared with Eppley Angstrom pyrheliometers, typical of which is the test at Table Mountain, California, on April 23, 1969. PACRADs II and III were compared with two pyrheliometers. The PACRADs agreed with each other within 0.11% and the pyrheliometers agreed with each other within 0.18%, with the pyrheliometers giving measured values of solar intensity 2.3% lower. Work is being done to resolve this discrepancy.

Appendix A

Correction Factors

This appendix is divided into two sections; the first is a brief discussion of view factors, and the second includes analyses of all recognized heat transfers in the radiometer. Correction factors are derived for those non-equivalent heat transfers of significant magnitude.

I. View Factors

When one part of the radiometer "sees" another part which differs in temperature, there is radiative exchange of heat between these parts. Quantitative information about the radiative exchange of the cavity through the cavity aperture with the view-limiting tube, muffler, and other parts of the radiometer can be obtained by making use of *view factors* (also called shape, form, or geometric factors). View factors are based on the purely geometric relationships involved with one surface placed in close opposition to another, taking into account the cosines of each area element with every other element viewed.

The view factor gives the fraction of an entire hemispherical field of view which one surface (the cavity aperture, in this case) "sees" of another surface or part. The amount of radiation entering the cavity from such a surface is given by

$$W_{in} = W_{2\pi} A_1 F_{1\text{-}2}$$

where

W_{in} = heat energy into irradiated surface, W/cm²

A_1 = area of radiating surface, cm²

$W_{2\pi}$ = equivalent hemispherical isotropic radiation, W/cm²

$F_{1\text{-}2}$ = view factor, surface 1 radiating to surface 2

Important for this work is the following formula to determine the view factor for one coaxial parallel circular disk with another disk (Ref. 5*):

$$F_{1\text{-}2} = \frac{1}{2}\left\{\frac{h^2+1}{r^2} + 1 - \left[\left(\frac{h^2+1}{r^2}+1\right)^2 - \frac{4}{r^2}\right]^{1/2}\right\}$$

$$r = \frac{r_1}{r_2}, \qquad h = \frac{h_1}{r_2} \tag{A-1}$$

*Formula can be found for example on p. 398 of referenced work.

Figure A-1 makes clear the geometric relationships occurring in this view-factor formula. This formula is used throughout this report to calculate view factors as needed.

The following general transformations are of use:

$$F_{1\text{-}2}\, A_1 = F_{2\text{-}1}\, A_2, \text{ or } F_{2\text{-}1} = F_{1\text{-}2}\frac{A_1}{A_2} \tag{A-2}$$

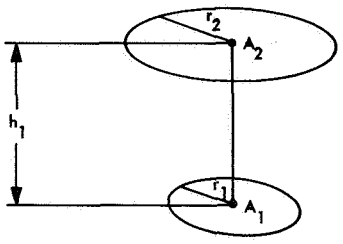

Fig. A-1. Geometric relationships for view factors

For radiative heat transfer between the view-limiting aperture and the cavity aperture (and between the view-limiting tube and the cavity aperture, where the view factors are small), a useful simplification of the equation can be obtained. This equation can be rewritten in terms of r_1, r_2, and h_1 as follows:

$$F_{1\text{-}2} = \frac{1}{2}\left\{\frac{h_1^2 + r_2^2 + r_1^2}{r_1^2} - \left[\left(\frac{h_1^2 + r_2^2 + r_1^2}{r_1^2}\right)^2 - \frac{4\, r_2^2\, r_1^2}{r_1^4}\right]^{1/2}\right\} \tag{A-3}$$

Let

$$h_1^2 + r_2^2 + r_1^2 = G$$

Then

$$F_{1\text{-}2} = \frac{G}{2\, r_1^2}\left[1 - \left(1 - \frac{4\, r_1^2\, r_1^2}{G^2}\right)^{1/2}\right] \tag{A-4a}$$

or

$$F_{2\text{-}1} = \frac{G}{2\, r_2^2}\left[1 - \left(1 - \frac{4\, r_2^2\, r_1^2}{G^2}\right)^{1/2}\right] \tag{A-4b}$$

When $4\, r_2^2\, r_1^2/G \ll 1$, it is easy to show that $F_{1\text{-}2} \cong r_2^2/G$ and $F_{2\text{-}1} \cong r_1^2/G$, where $G = h_1^2 + r_2^2 + r_1^2$.

II. Thermal Analysis

A. Thermal Coupling Between Cavity and Heatsink

The cavity, located inside the heatsink, is thermally coupled to the heatsink by three kinds of thermal coupling:

(1) Metallic conduction coupling (the principal part).

(2) Air conduction coupling.

(3) Radiative coupling.

Convection coupling might have been included, but it is insignificant due to the negligible difference of temperature, close spacing between cavity and heatsink, and relatively large viscosity of air. The heater winding on the cavity cone makes the electric heating closely equivalent to radiation heating. Even if there were convection effects, they would be the same for both radiation and electric heating and would cause no error. The metallic conduction coupling is provided by the thermal resistor, which is a silver cylinder. Most of the heat produced by irradiation of the cavity is conducted into the heatsink by the metallic coupling, here designated C_m.

Since the radiometer is not ordinarily evacuated, there is air filling the space between the cavity and the heatsink. This air causes an additional conductance, designated C_{air}. Finally, there is radiative coupling between the cavity and the heatsink. The outside surface of the cavity faces the inside surface of the heatsink, from which arises radiative coupling $C_{cav\text{-}hs}$. Also, the position of the cavity with respect to the inside parts of the muffler gives rise to radiative coupling $C_{cav\text{-}muf}$.

These two radiative thermal couplings, or conductances, can be lumped together to give the overall radiative coupling C_r: $C_{cav\text{-}hs} + C_{cav\text{-}muf} = C_r$.

The total thermal coupling C between the cavity and the heatsink is $C_m + C_{air} + C_r = C$. All heat produced in the cavity from absorption of radiation, or from electrical heating, must flow to the heatsink by conductance C.

When incoming heat W_{in}, coming either from radiation or from electric heating, flows from the cavity through the conductance C into the heatsink, a temperature drop ΔT occurs across the conductance. This drop may be expressed as $\Delta T = W_{in}/C$.

Precise values of C and ΔT are never known, and do not need to be known. By introducing the accurately known equivalent heating by the electric heater, however, the combination of the sensitivity of the thermopile and the magnitude of the conductance C can be calibrated. As has already been considered, use was made of the conductance C (reciprocal of thermal resistance) to obtain the calibration and working equation of the radiometer.

The combination of the overall effective magnitude of the thermal conductance between cavity and heatsink and the sensitivity of the thermopile gives an overall calibration factor which is obtained from equivalent electric heating. The magnitude of the heating effects, which are not equivalent to electric heating, is calculated and correction factors deduced to make allowances for them, so that measured values of radiation are corrected to give accurate determinations of measured radiation intensities.

B. Temperature Distribution in Cavity Cone With Radiative or Electric Heating

The cavity cone is heated either by incoming radiation or by electric heating to a temperature slightly higher than the temperature at the reference zone. As a result of this temperature increase, a slight increase of infrared radiation will escape through the cavity aperture.

The amount of escaping radiation will be computed for radiation heating and for electric heating. Any *difference* between radiation heating and electric heating is nonequivalent, and requires a correction factor. The temperature at the apex of the cone cavity is higher than the temperature at the reference zone. For each depth of the cone, the excess radiation can be computed by making use of the temperature distribution, and by using view factors, the excess radiation which escapes through the cavity aperture can be determined. The summation of excess escaping radiations from each zone depth h (x) gives the total infrared radiation which goes out through the cavity aperture.

Figure A-2 shows the cone, and how the various magnitudes are to be understood. The flux density at the outer edge of the cone (at $r = a$)

$$\frac{W_{in}\pi a^2}{2\pi at} = \frac{W_{in}a}{2t} \tag{A-5}$$

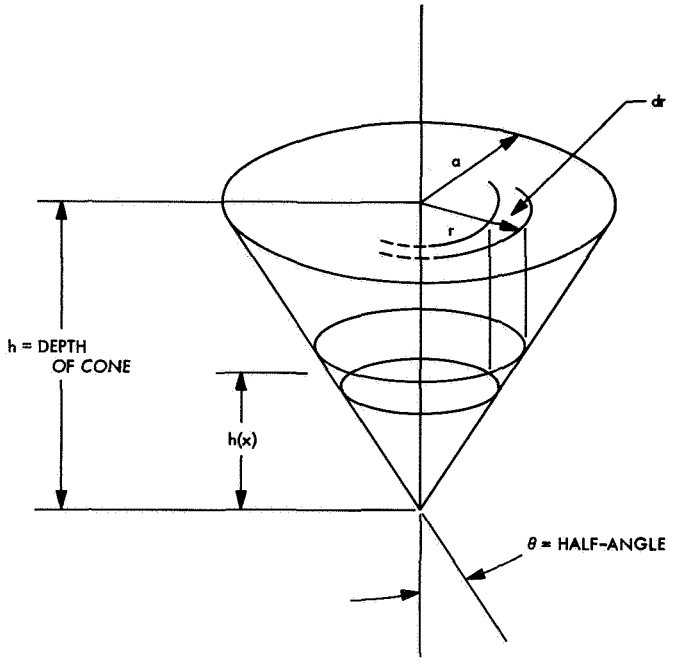

Fig. A-2. Conical portion of cavity

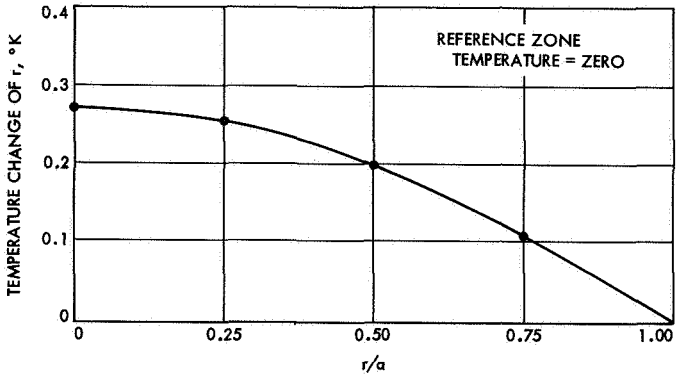

Fig. A-3. Temperature distribution in conical portion of cavity

The gradient at r is $W_{in}\, r/2 \sin\theta\, tK$ where

t = thickness of the silver in the cone

K = thermal conductivity of silver

W_{in} = collimated irradiance

a = radius of cone base

The temperature distribution (excess temperature over that at the reference zone) produced by this gradient is

$$\Delta T(r) = \int_r^a \frac{W_{in}\, r}{\sin\theta\, 2tK}\, dr = \frac{W_{in}\, a^2}{\sin\theta\, 4tK}\left(1 - \frac{r^2}{a^2}\right) \tag{A-6}$$

The excess radiation from $\Delta T(r)$ is

$$\Delta W = \frac{4A\epsilon\sigma T^4 F_{1-2}}{T}\, \Delta T(r) \tag{A-7}$$

Figure A-3 shows a plot of the distribution of Eq. (A-9) for these values:

$W_{in} = 0.100\ \text{mW/cm}^2$

$a = 0.563\ \text{cm}$

$t = 0.0127$

$K = 4.2$

$\sin\theta = 0.5$

$\sigma = 5.6697 \times 10^{-12}$

$T = 300°\text{K}$

$F_{1-2} = 0.100$

where A is $2\pi r\, dr$ and F_{1-2} is the view factor at r.

The excess radiation emitted as a function of the excess temperature at r is

$$\Delta W(r) = \frac{4A\epsilon\sigma T^4}{T}\, \Delta T(r) \tag{A-8}$$

Applicable values are

$\epsilon = 0.945$

$a = 0.563$

each $dr = 0.141\ \text{cm}$

which gives

$$\Delta W(r) = A\, 0.00058\, \Delta T$$

The total heat energy in watts escaping is

$$W = \sum \Delta W(r) \times 2\pi r\, dr\, F_{1-2} \tag{A-9}$$

From Eq. (A-9), it appears that the temperature distribution for the cone causes an addition of 7 μW of infrared radiation to escape through the cavity aperture for 100 mW/cm^2 irradiance of the cavity.

With regard to equivalence, however, the heater winding is so nearly in the same place as the inner

irradiated surface of the cavity cone that the temperature distribution with electric heating is virtually identical with that from radiation heating having the same power (also producing 7 μW). The main difference in heating comes about because of the small temperature drop from the heater wire to the silver substrate. According to investigative measurements, this drop for 100 mW of heating power is 0.1°K. The temperature of the silver substrate, however, is hardly reduced from what it would be if there were zero drop between wire and substrate. The wire is simply about 0.1°K hotter than it would be if the drop were zero. The main effect of the 0.1°K drop is that there is some extra heat transfer from the wire to the cone shield, due mostly to air conduction (but also to radiative emission of the wire).

The heat transfer from the wire to the cone shield is about 0.5% of the 100-mW heating power. Then $0.005 \times 100 = 0.5$ mW less flows in the conical portion of the cavity. The nonequivalent infrared radiation escaping from the surface through the cavity aperture is $0.05 \times 0.000007 = 0.035$ μW. This is the difference between the radiation heating and electric heating, and is small enough to be neglected.

All heat produced in the cavity, either by electric or by radiation heating, flows to the reference zone through the combined paths of the conical portion of the cavity and the cone shield. The electrical heating, except as noted just above, is therefore so nearly equivalent to radiative heating that no correction factor is required.

C. Effect of Temperature Distribution in Cavity Cylinder

During solar irradiation of the cavity, a certain amount of essentially solar spectral quality radiation is reflected from the irradiated inner surface of the cavity cone. Also, a certain amount of infrared radiation is emitted by the irradiated cavity cone coating due to the increased temperature of its surface (caused by the thermal resistance of the coating). Finally, as already shown, there is a temperature distribution in the silver substrate of the cavity cone in which the apex is at a higher temperature than the base. This increased temperature at the apex likewise contributes infrared emission, but the cavity cone temperature distribution is almost perfectly *equivalent,* as noted previously. The first two of the above-mentioned sources of radiant flux, which are *nonequivalent,* strike the cylindrical portion of the cavity and are absorbed there to set up a nonequivalent temperature distribution in the cylinder. The portion of the cavity involved in the following calculation extends from the reference zone in the cavity cylinder to the open end of the cavity.

With the temperature distribution in the cavity cylinder available, the air conduction and infrared emission from the cavity cylinder to the heatsink can be determined and appropriate correction factors deduced.

The reflected heat flux from the cavity cone depends primarily on the reflectivity of the coating in the cavity cone. The coating reflectivity is $1 - 0.98 = 0.02$. The enhancement of absorptivity by the cavity effect of the cone reduces the effective reflectivity to 0.01. For 100 mW into the cavity cone, 100 mW is reflected. The radiation emitted because of the coating thermal resistance was found to be 0.073 mW. The total flux from the cavity cone is 1.073 mW. Table A-1 includes the view factors from the cavity cone to the five zones of the cavity cylinder, and shows the amount of heat absorbed in each zone as $\Delta F_{1\text{-}2} A_1 W_{2\pi}$. From the summation of the individual heat fluxes, the temperature distribution in the cavity cylinder is obtained. The view factors were computed by means of the formula for disk-to-disk heat transfer. Table A-1 gives details and results of the computation where

$$\Delta T = Wh_1/AK = Wh_1/0.269$$

$$A = 0.064\ \text{cm}^2\ AK = 0.269$$

$$A_1 = 1\ \text{cm}^2$$

$$W_{2\pi} = 1.00 + 0.073\ \text{mW} = 1.073\ \text{mW}$$

For nonequivalent (perturbation) temperature distributions, the reference zone is always considered to be at zero. The temperature distribution given in Table A-1 covers the cavity cylinder which extends from the reference zone to the open end of the cavity.

D. Heat Transfer by Air Conduction—Cavity Cylinder to Heatsink

With the availability of the values for temperature distribution in the cavity cylinder from solar irradiation, the heat transfer can be computed for air conduction from the cavity cylinder to the heatsink. The heat flux from each zone of the cavity cylinder can be obtained by means of the heat flow field in the air between the cavity and the heatsink. But mapping of the flow field for the geometry of the cavity cylinder surrounded by the heatsink is difficult to do by mathematic analysis. It is nevertheless simple to obtain a rough graphical solution suggested by Laplace's equation ($\nabla^2 T = 0$ for steady-state condition), which gives sufficient accuracy for the purpose.

Table A-1. Temperature distribution

h_1 zone	h_1 midpoint	ΔF_{1-2}	$\Delta F_{1-2} A W_{2\pi}$	$h_1 = 0.1695$	$h_1 = 0.5645$	$h_1 = 0.985$	$h_1 = 1.28$	$h_1 = 1.5$
0.000 0.339	0.1695	0.2323	0.249	0.0001565	0.0001565	0.0001565	0.0001565	0.0001565
0.339 0.790	0.5645	0.3303	0.354	0.000223	0.000742	0.000742	0.000742	0.000742
0.790 1.18	0.985	0.1596	0.172	0.0001078	0.000358	0.000627	0.000627	0.000627
1.18 1.38	1.28	0.0976	0.105	0.000659	0.000210	0.000383	0.000500	0.000500
1.38 1.63	1.50	0.0807	2.087	0.000545	0.000182	0.000317	0.000412	0.000483
Computed totals		0.90054 ΔF_{1-2}	0.967 mW	0.000606°K $= \Delta T$ at $h_1 = 0.1695$	0.00166°K $= \Delta T$ at $h_1 = 0.5645$	0.00222°K $= \Delta T$ at $h_1 = 0.985$	0.00243°K $= \Delta T$ at $h_1 = 1.28$	0.00251°K $= \Delta T$ at $h_1 = 1.5$

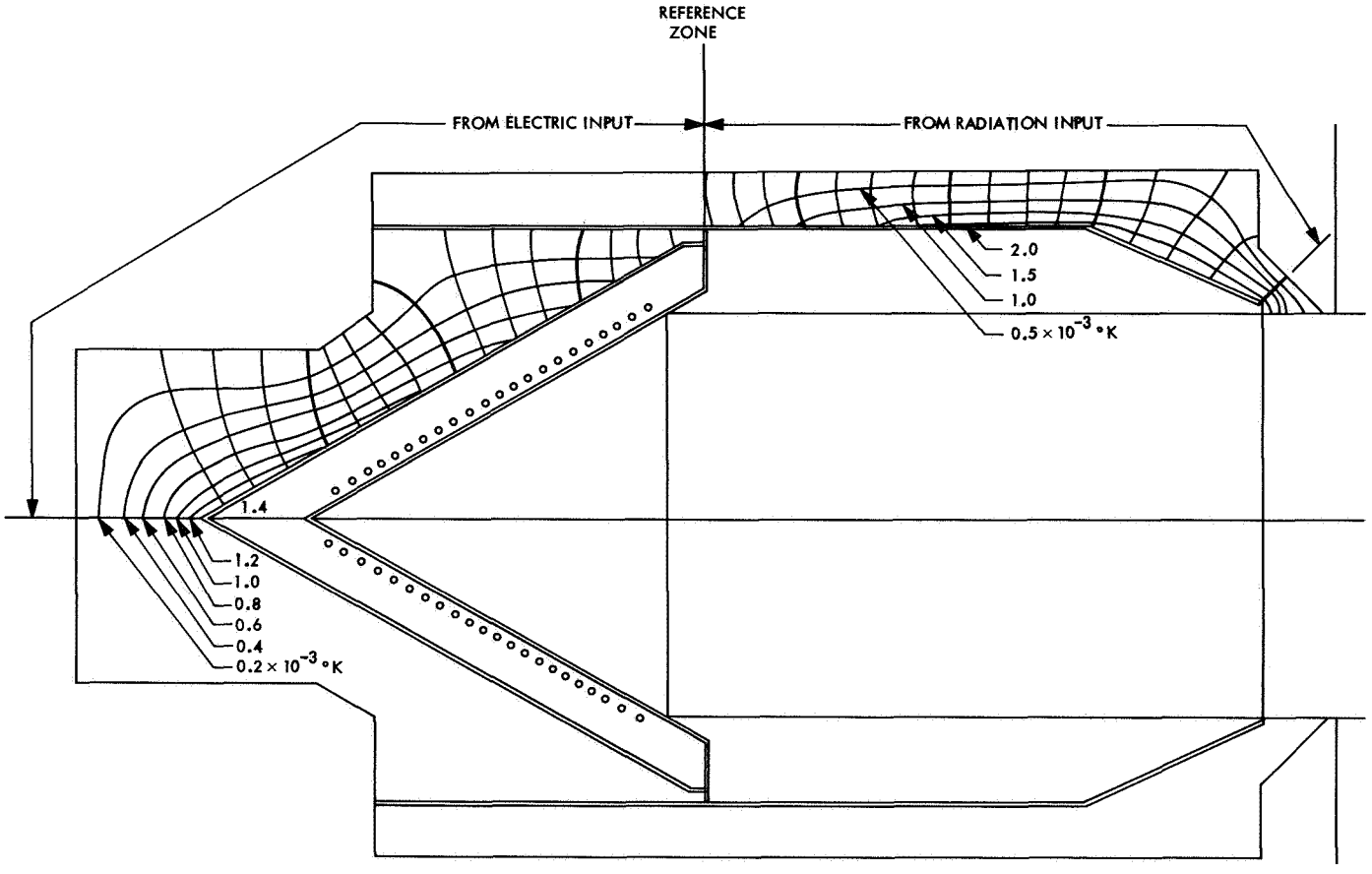

Fig. A-4. Nonequivalent heat transfer by air conduction

Figure A-4 shows this geometry, with heat flux lines and isothermal surfaces sketched in. The heavy heat flux lines indicate boundaries of the various regions used for summing the heat flows from the various parts of the cone shield to the thermal resistor and to the heatsink. The isothermal surfaces are also sketched in, and they, of course, are normal to the heat flux lines.

It must be remembered that this plot is for the perturbation, or nonequivalent, portion of the total heat transfer from the cavity cylinder and cone shield to the thermal resistor and heatsink. The *equivalent* heat transfer is so much greater that if the total heat flow pattern were plotted, there would scarcely be a recognizable difference in the appearance from the addition of the nonequivalent heat flow.

Figure A-4 shows not only the flow field for the cavity cylinder to the heatsink, but the flow field for the cone shield to the heatsink. From the flow field it is possible to estimate the thermal gradients around the cavity cylinder. From the thermal gradients dT/dx and the zonal area A the heat transfer W for each zone is obtained as $AK(dT)/dx = W$, where K is the thermal conductivity of air, and dT/dx is the thermal gradient. The summation of these individual heat transfers gives the total air conduction heat energy (in watts) from the cavity cylinder to the heatsink for 100 mW/cm² irradiance. Table A-2 gives the numerical values of the computation.

E. Radiative Heat Transfer—Cavity Cylinder to Heatsink

Since the radiative heat transfer from the cavity cylinder to the heatsink is quite small, a rough estimation of its magnitude is all that is necessary. The external area of the cavity cylinder is $\pi \times 1.63$ cm (diameter) $\times$ 1.63 cm (length) = 8.35 cm². The maximum temperature difference is $\Delta T = 0.0025°K$. The emissivity ϵ can reasonably be assumed to be 0.3. The radiative heat transfer from the cavity cylinder to the heatsink then is

$$\Delta W = \frac{A\epsilon 4\sigma T^4 \Delta T}{T} \qquad \text{(A-10)}$$

with

$$\sigma T^4 = 46\,\text{mW/cm}^2$$

$$T = 300°K$$

$$\Delta T = 0.0025°K$$

$$A = 8.35\,\text{cm}^2$$

Thus, $W = 0.0038$ mW, and $Cf = 1 + 0.0038/100 = 1.00004$.

F. Infrared Radiation Emitted From Aperture by the Inner Surface of Cavity Cylinder

The infrared radiation emitted through the aperture by the inner black surface of the cavity cylinder due to the nonequivalent temperature distribution in the cylinder was estimated from the nonequivalent temperatures in the cylinder to give the local radiosity of each of the five local zones. View factors from these zones to the cavity were calculated, and the amount of radiation going out through the aperture from each zone was obtained from the formula $W = A_1 F_{1-2}\, W_{2\pi}$, where $W_{2\pi} = 4\epsilon\sigma T^4 \Delta T/T$. The resultant values are given in Table A-3.

The heat transfer by air conduction was found to require a correction factor of 1.00023 and the radiation out through the cavity aperture from the cavity cylinder was found to require a correction factor of 1.00002.

Table A-2. Air conduction—cavity cylinder to heatsink

h_1 (midpoint), cm	$T(h_1)$, °K	dT/dx, °K/cm in air	Zonal area A, cm²	$AK\frac{dT}{dx}$, = μW[a]
0.1695	0.000606	0.00413	2.02	2.00
0.5645	0.00166	0.01073	2.02	5.20
0.985	0.00222	0.0134	2.02	6.43
1.28	0.00243	0.0134	1.18	3.80
1.50	0.00251	0.0214	1.00	5.14

[a]Total $AK(dT/dx) = 0.0226$ mW; the correction factor $Cf = 1 + 0.0226/100 = 1.000226$ or, rounded off, 1.00023.

Table A-3. Infrared radiation

h_1[a]	F_{1-2}	ΔT, °K	Irradiance $W_{2\pi}$ μW	Heat transfer[b] W, μW
0.16	0.6285	0.0023391	1.3	0.9
0.36	0.3994	0.0022726	1.3	0.5
0.65	0.2617	0.002076	1.3	0.5
1.06	0.1602	0.001548	0.8	0.2
1.45	0.1059	0.000567	0.3	0.0

[a]$h_1 = 0$ is at the aperture.
[b]Total $W = 0.0021$ mW, so correction factor $Cf = 1 + 0.0021/100 = 1.00002$.

The overall correction factor Cf due to cavity cone reflection heating of the cavity cylinder, involving air conductive and radiative heat transfer from the cone cylinder and emission from the aperture, is $1.00023 \times 1.00004 \times 1.000002 = 1.00029$.

G. Radiative Heating of Cavity Aperture Limiter

The view-limiting tube and the muffler have been arranged so that no direct radiation falls on any of the radiation diaphragm stops mounted in the muffler. As a result, there is no heating by direct radiation of these parts of the radiometer. However, the view-limiting aperture has about double the area of the cavity aperture, which thereby permits introduction of about 100% more radiation into the radiometer than into the cavity. This excess radiation, excluded from the cavity by the cavity aperture limiter, is 98% absorbed by its blackened surface. The heat thus absorbed is conducted through the cavity aperture limiter into the radiometer heatsink, except for a small amount transmitted through the thickness of the limiter and reradiated (and air-conducted) into the cavity. This nonequivalent heat flux requires a correction factor.

An approximate calculation—taking into account the dimensions of the cavity aperture limiter, its thermal conductance (3.9 W/cm²/cm/°K), and the amount of heat absorbed by it (0.098)—shows that the temperature of the inner edge of the cavity aperture is about 0.01°K higher than the temperature of the heatsink. Assuming a reasonable area for the reradiating surface (1.0 cm²), emissivity ($\epsilon = 0.1$), and a view factor of 0.7, the nonequivalent heat transmitted and entering the cavity is <1.0 μW, small enough to be neglected.

Figure A-5 shows a flow field diagram of the heat flow in the copper cavity aperture limiter and in the air between the limiter and the open end of the cavity. As indicated by the following rough calculation, it is hardly necessary to estimate in complete detail the heat flow from the limiter to the cavity since the flux is so small. Even a 50% error in the estimation causes less than 0.01% error in the overall accuracy of the radiometer.

For the air conduction from the cavity aperture limiter to the cavity, the approximate area of the conductive path is 1 cm². The effective length is about 0.12 cm. The resulting temperature gradient in the air is 0.005°K/0.12 cm or 0.0416°K/cm. The air conduction, $AK(dT)/dx$ is $1 \times 0.24 \times 0.0416 = 0.010$ mW for an irradiance of 100 mW/cm². The correction factor Cf is $1 - 0.01/100 = 0.99990$.

H. Rereflected Radiation From Muffler Into Cavity

The black cavity aperture limiter reflects about 2.0% of the radiation falling on it. The intensity of the incoming radiation is 100 mW/cm² and the area of the beam intercepted by the cavity aperture limiter is about 1 cm². Of the reflected radiation (100×1 cm² $\times 0.02 = 2.0$ mW), some 41% is passed through the hole in the muffler diaphragm stop, and 59% is intercepted by the stop, according to calculated view factors. The stop, also painted black, has a reflectivity of about 0.02. Of this rereflected radiation, about 40% is returned through the cavity aperture to the cavity, where it reinforces the direct incoming radiation. The amount of reinforcement is $2.0 \times 0.59 \times 0.02 \times 0.4 = 0.0094$ mW from an irradiance of 100 mW/cm². A correction factor is required to make allowance for the nonequivalent reinforcing radiation: $0.0094/100 = 0.000094$; corresponding correction factor Cf is $1 - 0.00009 = 0.99991$.

I. Nonequivalent Heat Flow, Cone Shield to Heatsink With Electric Heating

The wire of the heater winding on the conical portion of the cavity is about 0.1°K hotter than the silver substrate. About 0.5% of the heat generated by electric

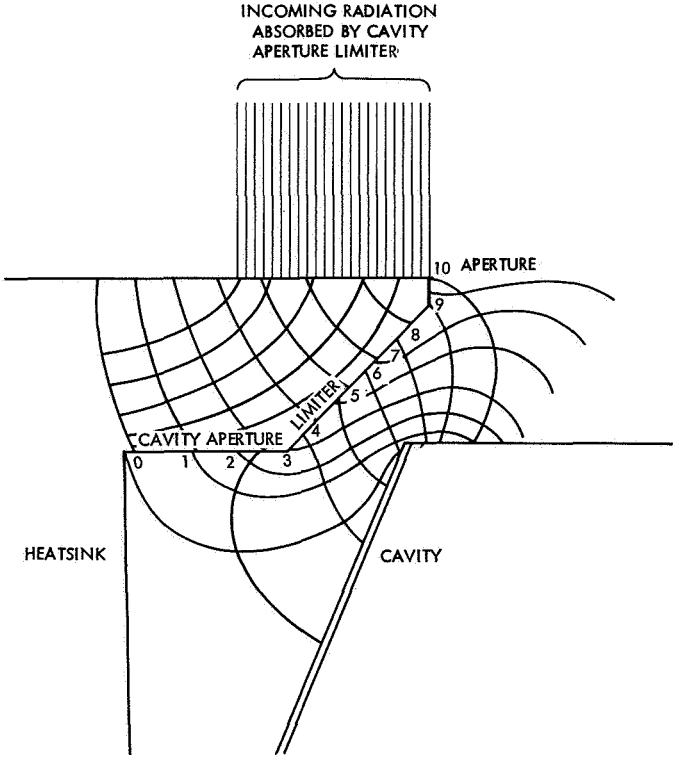

Fig. A-5. Nonequivalent heat transfer by air conduction around aperture

heating gets conducted by air and radiation into the cone shield. The temperature distribution in the cone shield, then, is similar to that in the conical portion of the cavity, but it is only about 0.5% as large. The temperature at the apex of the cone shield is about 0.0014°K above that at the reference zone.

Since the outside surface of the cone shield is polished silver, it has negligible nonequivalent radiant emission from the 0.0014°K at the apex. The air conduction, however, is not negligible.

When 100 mW of electric heating is applied to the cavity cone, the wire of the electric heater runs about 0.1°K higher than the silver substrate in the cavity cone because of thermal resistance of the electrical insulation for the wire. The extra heat transfer from the 0.1°K temperature takes place from the wire to the cone shield to make it a little hotter. Then air conduction between cone shield and heatsink causes some of this heat to bypass the thermal resistor and go directly to the heatsink, thereby introducing nonequivalence.

The cone shield can be divided into the four regions shown by the heavy heat flow lines in Fig. A-4. The average temperature gradient in the air in each region can be estimated from the plot of Fig. A-6. In each region, the heat flux is

$$W = \frac{\Delta T}{l} AK \qquad \text{(A-11)}$$

where $\Delta T/l$ = temperature gradient in degrees (Kelvin) per centimeter for the region, and K = thermal conductivity of air (0.24 mW/cm²/cm/°K).

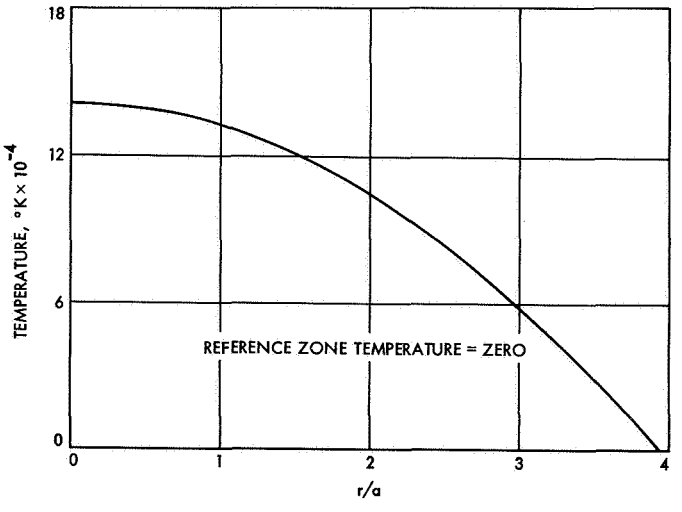

Fig. A-6. Temperature distribution in cone shield

Carrying this procedure through (using the four regions shown) indicates that the total nonequivalent heat transfer from the cone shield to the thermal resistor and to the heatsink is 0.0045 mW for 100 mW of electric heating. The corresponding Cf is $1 - 0.0045/100 = 0.999955$.

It takes a little time for the steady-state temperature distribution in the air between the cavity and the heatsink to be attained. Air has low thermal mass per cubic centimeter but it also has low thermal conductivity. The thermal diffusivity of air, however, is surprisingly high (0.187)—about 1.5 times that of steel. In the absence of convection, thermal disturbances are propagated wavelike through air about one-fifth as rapidly as through copper. A rough idea of the maximum possible time required to establish the steady-state temperature field in the air around the cone shield can be obtained by basing the computation on the longest distance between the cone shield and the thermal resistor. This distance is about 0.5 cm. From the computer-compiled data in Table A-4, the temperature will be established to closer than 99% of the final value when $Kt/l^2 = 1.98$, or

$$t = \frac{1.98\, l^2}{K} = \frac{1.98\,(0.5)^2}{0.187} = 2.8 \text{ s}$$

Table A-4. Heat transfer (cone shield to heatsink) from radiation input

Slant height zone, r/a	Zonal area, cm²	dT/dx in air	Heat transfer[a] $W = AK\frac{dT}{dx}$, μW
0–0.4	0.251	0.0100	0.602
0.4–0.8	0.75	0.0070	1.26
0.8–1.2	1.26	0.0040	1.20
1.2–1.6	1.76	0.0033	1.40

[a]Total heat transfer = 4.46 μW.

This time is short compared to the 56 s for the cavity thermal resistance system. For all practical purposes, the temperature field in the air is always in the steady-state condition, even while the cavity is undergoing a change of temperature.

J. Effect of Nonisothermality in View-Limiting Tube and Muffler

The view-limiting tube is not necessarily at the same temperature as that of the heatsink. If there is a difference, there will be a radiative exchange between the

view-limiting tube and the cavity. An estimate of the magnitude of the effect must be made to determine its importance.

The radius of the muffler top diaphragm stop is $r_1 = 1.1125$ cm, $h_1 = 8.2550$ cm, and $r_2 = 0.642$ cm. So

$$G = h_1^2 + r_1^2 + r_2 = 68.145 + 0.3183 + 1.1238 = 69.701$$

$$F_{1-2} = \frac{r_2^2}{G} = \frac{0.3183}{69.701} = 0.004567$$

This is the view factor of the top of the muffler to the cavity aperture. The view factor of the view-limiting aperture to the cavity aperture is

$$F_{1-2} = \frac{r_2^2}{G} = \frac{0.3183}{363.88} = 0.000876$$

where

$$G = h_1^2 + r_1^2 + r_2^2$$
$$= 362.902 + 0.6606 + 0.3183$$
$$= 363.88$$

$$\Delta F_{1-2} = (F_{1-2})_{muf\,ap} - (F_{1-2})_{VL\,ap}$$
$$= 0.004567 - 0.000876 = 0.0036909$$

The radiative transfer is

$$W = W_{2\pi}\,\Delta F_{1-2} A_1 \qquad \text{(A-12)}$$

where A_1 = area of top of muffler = 3.88 cm². As an example, assume that the view-limiting tube is 5°K hotter than the temperature of the heatsink and cavity. Then

$$W = \frac{0.046 \times 4 \times 0.0036909 \times 3.88 \times 5}{300}$$
$$= 0.000044 \text{ W, or } 0.044 \text{ mW}$$

Thus, when the view-limiting tube is 5°K hotter than the heatsink (and cavity), the view-limiting tube transfers 0.044 mW into the cavity. If $\Delta T = 10$°K, the radiative transfer is 0.088 mW.

This does not represent error, unless the temperature at the measurement of an incoming intensity has changed 5 or 10°K (respectively) from the temperature at calibration. If this happens, and no allowance is made, the error would be

$$\frac{0.088}{100} = 0.00088$$

which is almost 0.1% for a 10°K change.

A 10°K excess temperature of the view-limiting tube would cause a thermopile offset emf

$$\Delta v = \frac{\Delta W}{K} = \frac{0.088}{0.1800} = 0.49\,\mu\text{V}$$

where

K = calibration constant

This offset would cause only an insignificant error in the measurement, as can be seen from Fig. 9, showing a plot of $W_{in\,(apparent)}/W_{in\,(true)}$ vs v/v_{cal}. Thus it appears that if the temperature of the view-limiting tube differs from that of the heatsink by 10°K, and remains constant from calibration to measurement, it will cause no error.

K. Radiation From Cavity Lost to External Space

When external space is at 0°K, no radiation from external space enters the cavity. The cavity, being at about 300°K, however, is always (no matter what is coming in) emitting radiation through the cavity aperture and view-limiting aperture to external space. A correction for this loss of radiative power must be made.

Since the view factor of the cavity aperture to the view-limiting aperture is small, it is permissible to use the approximate simplified expression given in Appendix A-1 about view factors:

$$F_{1-2} = \frac{r_2^2}{G} \qquad \text{(A-13)}$$

where

$$G = h_1^2 + r_1^2 + r_2^2$$

The area A_1 of the cavity aperture is 1 cm², and the temperature is 300°K. For the 5-deg acceptance angle,

$h_1 = 19.050$

$r_1 = 0.8128$ cm

$r_2 = 0.564$ cm

$G = 362.9025 + 0.3183 + 0.66064 = 363.88$

$$F_{1-2} = \frac{r^2}{G} = \frac{0.66064}{363.88} = 0.001815$$

$$W_L = W_{2\pi}\,F_{1-2}\,A_1 = 0.046 \times 0.001815 \times 1$$
$$= 0.0000834 \text{ W, or } 0.0834 \text{ mW}$$

for a 5-deg acceptance angle. This much radiative power, W_L, is being emitted at all times from the cavity, and must be added to every measured value of intensity obtained.

If the acceptance angle is increased to 8.17 deg ($r_2^2 = 1.8535$), the view factor is

$$F_{1\text{-}2} = 0.005077$$

$$W_L = W_{2\pi} F_{1\text{-}2} A_1$$

$$= 0.046 \times 0.00508 \times 1 = 0.000234\ \text{W}\ (0.234\ \text{mW})$$

For various acceptance angles, W_L is

Acceptance angle, deg	W_L, mW/cm²
5	0.0834
8	0.230
15	0.80

Also, as the heatsink temperature changes, so would $W_{2\pi}$, thus making a corresponding change in W_L.

L. Nonequivalent Temperature Distribution in the Muffler (Electric Heating)

About 200 mW enters the view-limiting aperture (area = 2 cm²) when the irradiance is 100 mW/cm². Half this amount goes directly into the heatsink via the cavity aperture limiter, and the other half enters the cavity, all of which goes to heat the heatsink and muffler at a rate of 0.0001952°K/s. When electric heating is used for calibration, only 100 mW goes to heat the heatsink (at a rate of 0.0000976°K/s). The difference, also 0.0000976°K/s, makes for a nonequivalence.

The muffler, which is thermally joined to the heatsink, is essentially cylindrical, and thermally can be considered as a bar, one end of which is heated at a rate of 0.0000976°K/s. A nonequivalent temperature distribution results, with the top end cooler than the end at the heatsink. The muffler then receives nonequivalent irradiance from the cavity. An outline of the calculations for this nonequivalence is given below. The amount of nonequivalence was found to be negligible.

The steady-state rate of heat absorption at x cm from the heatsink end of the muffler is

$$\frac{\rho c\, A\, dx}{AK} \frac{dT}{dt} = \frac{1}{k} \frac{dT}{dt}\, dx \qquad \text{(A-14)}$$

where k is the thermal diffusivity for copper, K is the thermal conductivity of copper, and A is the cross-sectional area of the muffler.

The thermal gradient at x is

$$dT/dx = \frac{W_{2\pi}}{AK} \int_{x/L}^{1} \frac{dx}{L} = \frac{W_{2\pi}}{AK} \left(1 - \frac{x}{L}\right) \qquad \text{(A-15)}$$

The integral of this gives the nonequivalent temperature distribution in the muffler

$$\Delta T = \frac{W_{2\pi} L}{AK} \int_x^L \left(1 - \frac{x}{L}\right) dx = \frac{W_{2\pi} L}{AK} \left(\frac{x}{L} - \frac{1}{2} \frac{x^2}{L^2} + c\right) \qquad \text{(A-16)}$$

where $x/L = 0$, $\Delta T = 0$, and $c = 0$.

Figure A-7 shows a plot of the distribution in the muffler. The temperature of the top end of the muffler is 0.0024°K cooler than the temperature of the heatsink.

A rough estimation of the nonequivalent radiance of the cavity is sufficient to show that the nonequivalent emitted radiation from the cavity is negligible.

Assume that the entire muffler is at two-thirds the end temperature ($2/3 \times 0.0024°\text{K} = 0.0016°\text{K}$); the view factor from the cavity to the muffler is 1. The nonequivalent radiation is

$$\Delta W = \frac{4A\sigma T^4\, dT}{T} \qquad \text{(A-17)}$$

where

$$\sigma T^4 = 46\ \text{mW/cm}^2$$

$$T = 300°\text{K}$$

$$A = 1\ \text{cm}^2$$

$$dT = 0.0016$$

$$\Delta W = \frac{4 \times 1 \times 46 \times 0.0016}{300} = 0.001\ \text{mW},$$

a negligible amount.

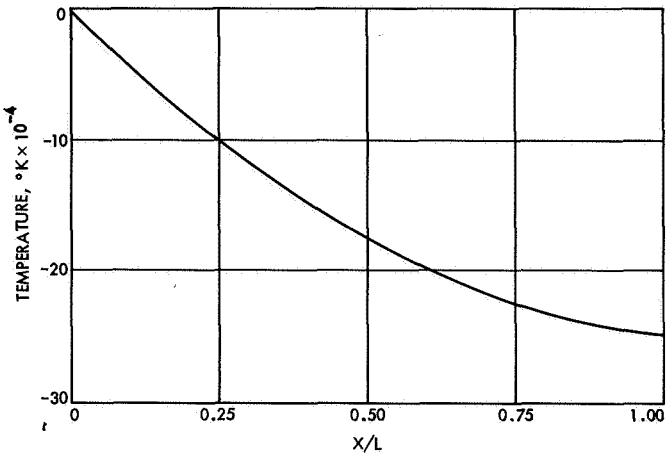

Fig. A-7. Nonequivalent temperature distribution in muffler

Appendix B

Heatsink Constants

Material of heatsink = copper, $\rho = 8.94$, $K = 0.93 \times 4.2 = 3.9$, $c = 0.0914 \times 4.2 = 0.384$, $k = 1.14$

Weight of heatsink = 2665 g

Weight of muffler alone = 680.4 g

Cross-sectional area of muffler = 10.0 cm²

Height of muffler = 7.6 cm

Heat capacity of total heatsink = $cM = 2665 \times 0.0914 \times 4.2 = 1023$ W-s/°K

Heat capacity of muffler alone = $680.4 \times 0.0914 \times 4.2 = 261.2$ W-s/°K

Muffler fraction of total mass M 680.4/2665 = 0.255, or 25.5%

Thermal conductance of muffler (for 1 cm of length) $AK = 10 \times 0.93 \times 4.2 = 39.05$ W/cm/°K

Area of hole in cavity aperture limiter = 1.000584 cm²

Muffler stabilization time, 1 time constant (to within 37%) = 14.6 s
(to within 99%) = 100 s

Thermal guard stabilization time is equal to muffler stabilization time.

The overall weight of the above radiometer is almost 14 lb. The new radiometer, which uses magnesium for nearly all metal parts, weighs 2.2 lb.

Appendix C

Offset Considerations

If there is an offset emf Δv produced by the thermopile, which, e.g., might be caused by: (1) the view-limiting tube having a temperature differing from that of the cavity, (2) a parasitic thermal emf produced anywhere in the circuit, (3) a zero reading of the nullmeter, or (4) produced by any other cause, there will be an error in the measurement intensity unless a calibration is taken with a heating power closely approximating the power of the irradiance being measured. The calibration emf V_{cal} should be nearly equal to the emf produced by the irradiance; that is, $v_{cal} \approx v$. In the following, the effect of power losses W_L is neglected:

If $\Delta v = 0$, then the true $W_{in} = Kv$, where the constant $K = (EICf)/v_{cal}$. If $\Delta v \neq 0$, the apparent $W_{in} = K_{\Delta v \neq 0}$ $(v + \Delta v)$, where $K_{\Delta v \neq 0} = (EICf)/(v_{cal} + \Delta v)$, which is equivalent to W_{in} as measured.

It is assumed that Δv at measurement is equal to Δv at calibration. The following ratio indicates how much error might be caused by the emf offset:

$$\frac{W_{in\,(apparent)}}{W_{in\,(true)}} = \frac{EICf}{v_{cal} + \Delta v} \cdot \frac{v_{cal}}{EICf} \frac{(v + \Delta v)}{v}$$

$$= \frac{v_{cal}}{v} \frac{v + \Delta v}{v_{cal} + \Delta v} = \frac{1 + \dfrac{\Delta v}{v}}{1 + \dfrac{\Delta v}{v_{cal}}}$$

$$\cong 1 + \left(1 - \frac{v}{v_{cal}}\right) \frac{\Delta v}{v} \qquad \text{(C-1)}$$

Figure C-1 is a plot showing the relationship of $W_{in\,(apparent)}/W_{in\,(true)}$ to v/v_{cal} for $\Delta v = 0.002$, 0.001, and 0.0005 mV. The recommended operating range is $0.9 < v/v_{cal} < 1.1$, in which even $\Delta v = 0.002$ mV produces an error in the measurement of less than 0.05%, when the measured intensity is 0.100 W/cm². It is assumed that Δv at measurement is equal to Δv at calibration. These operating constraints are easily satisfied in actual operation.

The effect of Δv can usually be ignored when making a measurement. Thus, Eq. (C-1) becomes

$$W_{in} = \frac{EICf}{v_{cal} + \Delta v} (v + \Delta v) + W_L \qquad \text{(C-2)}$$

The values for $(v_{cal} + \Delta v)$ and $(v + \Delta v)$ represent total electromotive-force values which can be directly read out on the digital voltmeter.

Although Eq. (C-2) does not take into account the voltage offset, it can be used as given since it will implicitly include Δv and Δv_{cal} in v and v_{cal} in the values read out (see also curves of Fig. C-1).

Direct readout in W/cm², W/ft², or J/cm²/min can easily be provided for by adjusting the sensitivity of the electronic circuit and recording instrument to give any of the above units of intensity.

Johnson (thermal) noise is generated by any resistor which has an absolute temperature greater than zero. The thermopile has about 100-Ω resistance and operates at a temperature of about 300°K. Its Johnson noise, however, is negligibly small, as shown below.

The Johnson noise is given by the expression

$$v = (4kTR\Delta f)^{1/2} \qquad \text{(C-3)}$$

where

v = Johnson noise in volts from the resistance

R = resistance in ohms (100 Ω)

T = temperature in degrees Kelvin (300°K)

k = Boltzmann constant (1.380×10^{-9} W-s/°K)

Δf = passband of electronics in Hz (10 Hz)

The above values substituted in the formula indicate a Johnson noise of 0.005 μV, which is negligible compared to the thermopile output of, say, 0.5 mV.

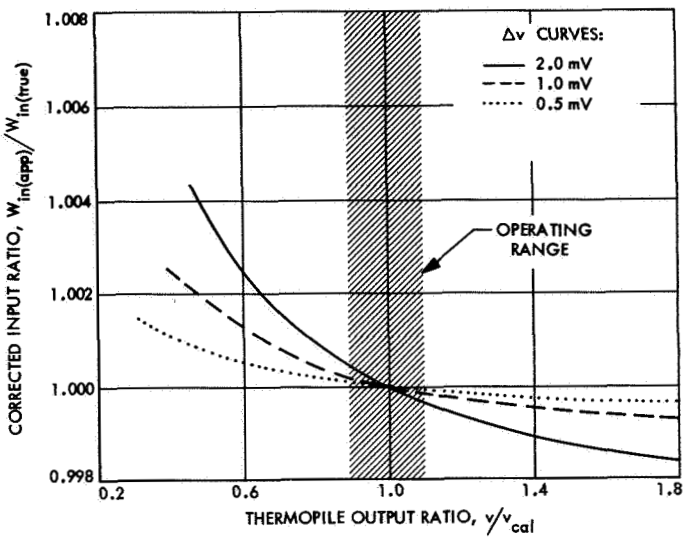

Fig. C-1. Effect of Δv and Δv_{cal} on $W_{in(app)}/W_{in(true)}$

Appendix D

Time Constants

I. Time Constant of the Cavity and Thermal Resistance System

The effective thermal resistance associated with the cavity is composed of the metallic thermal resistor, air conduction between cavity and heatsink, and radiation coupling of the cavity with the heatsink. The cavity has heat capacity which, with the effective thermal resistance, determines the time constant of the cavity and thermal resistance system. This time constant determines the time response to, say, a step function of either electric heating or incoming radiation heating, and indicates how long one must wait before an accurate reading of intensity (or electric heating) can be obtained.

The effective thermal resistance can be ascertained by applying a known amount of electric heating to the cavity and measuring the temperature drop across the effective thermal resistance. The thermopile is made up of 18 pairs of Chromel–Constantan thermojunctions, each with a sensitivity of about 60 μV/°K.

Assume 100 mW electric heating is applied to the cavity, and causes the thermopile to generate an output of 850 μV. Each thermojunction then generates $\frac{1}{18} \times 850 = 47$ μV. The temperature drop across the thermal resistance is $47/60 = 0.8$°K. An input of 1 W would give 8°K which indicates that the effective thermal resistance is 8°K/W, or $R = 8$ "thermal ohms."

The heat capacity of the cavity can only be estimated. The effective weight of the cavity is about 3 g, and the specific heat of silver is 0.05—$0.05 \times 4.2 = 0.21$ W-s/°K/g. The heat capacity of the cavity is $c = 3 \times 0.21 = 0.63$ W-s/°K. The indicated time constant RC is $8 \times 0.63 = 5$ s.

The actual time constant determined from a measurement was found to be 7 s. The extra 2 s could be coming from the heat capacity of the electrical insulation of the heater winding and thermopile for which no allowance was made in the above estimation.

It is not necessary to know the time constant accurately, but it is necessary to know the *combined* value of the effective thermal resistance and the thermopile sensitivity with the greatest accuracy possible. In effect, this value is implicitly determined very accurately every time the calibration constant K is obtained.

Table D-1 gives the response of the cavity and thermal resistance system in terms of $1 - (1/e)$ time constants and the degree of thermal stabilization. If, after applying the step function of heating, one waits 55 s (8 time constants of 7 s each), the system has stabilized to 99.997% of its final value. In other words, it takes about 1 min for the radiometer to come to its final reading.

Table D-1. Response time in terms of 1 — (1/e) time constants

Number of time constants	e^{-x}	$1-e^{-x}$	Time, s
x	—	—	—
0	1.000	0.000	0
1	0.368	0.632	7
2	0.13533	0.8647	14
3	0.0498	0.9502	21
4	0.0183	0.9817	28
5	0.00674	0.9932	35
6	0.00248	0.9975	42
7	0.000912	0.9991	49
8	0.0000335	0.99997	56

II. Time Constant for Temperature Stabilization of the Muffler Temperature Distribution

The effect of the steady-state temperature heating of the muffler has already been considered. The effect of the nonsteady state must be considered to determine its importance. It is of course desirable to have rapid attainment of the steady state because until then no accurate measurements can be made. It is necessary to determine how long one must wait for this after a heating change occurs before taking a measurement reading.

The muffler can be considered as a bar, one end of which is in intimate contact with the heatsink. If the heatsink suddenly changes temperature, the bar (muffler) follows, but with various amounts of delay distributed along its length, with the most temperature delay occurring at the free end. The muffler is made of copper, so that, except for silver and gold, it has the highest thermal diffusivity of all metals. On this account, the temperature changes of the heatsink are followed rapidly.

To get quantitative information, it is simplest to consider the temperature as a function of time at the top end of the muffler when a step function change of temperature has been applied to the bottom end. The solution to this problem is given by Carslaw and Jaeger (Ref. 6).

The function u/u_o (nondimensional temperature function) is given as a series with the independent variable kt/l^2, where k = thermal diffusivity, t = time in seconds, l = length of the bar in centimeters:

$$u/u_o = 1 - \frac{4}{\pi}\left[\exp\left(-\frac{\pi^2}{4}\frac{kt}{l^2}\right) - \frac{1}{3}\exp\left(-\frac{9\pi^2}{4}\frac{kt}{l^2}\right) + \frac{1}{5}\exp\left(-\frac{25\pi^2}{4}\frac{kt}{l^2}\right) - \cdots\right] \quad \text{(D-1)}$$

The substituting of values in this series is long and tedious. On this account, the IBM 7090 computer was used to prepare a complete table of values up to $kt/l^2 = 3$. Figure D-1 shows a plot of this function. The value of most interest is that for u/u_o, for the so-called time constant $1/e = 37\%$, for which

$$kt/l^2 = 0.29$$

$$t = 0.29\, l^2/k$$

$$= \frac{0.29 \times 57.7}{1.14} = 14.6 \text{ s}$$

Also of interest is the value for $u/u_o = 0.99$, for which

$$kt/l^2 = 1.98$$

$$t = 100 \text{ s} = 1\tfrac{2}{3} \text{ min}$$

In summary, if one waits a few minutes after the thermal guard (heatsink) has a change of temperature, no discernible error should be expected from lack of stabilization of the muffler temperature distribution.

Even if one does not wait this long, the error will ordinarily still be small enough to be neglected. The principal reason for making this computation is for knowing the general order of magnitude of the stabilization time.

It is also worth noting that the heatsink is nearly of the same length as the muffler; hence, its stabilization time is also nearly the same.

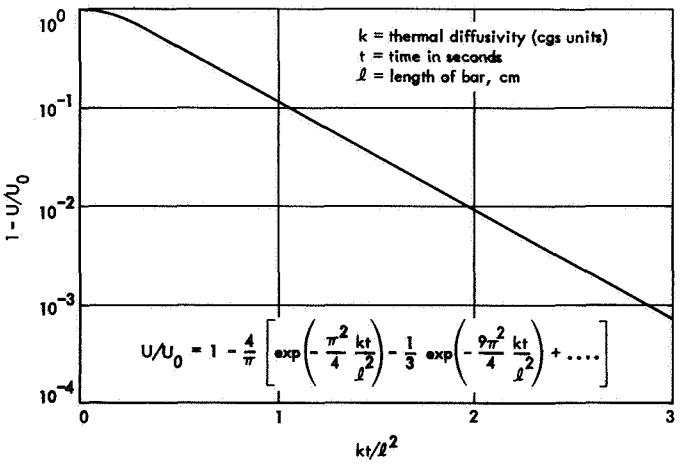

Fig. D-1. Temperature of end of bar vs time, thermal diffusivity, and length

Nomenclature

A	area
a	cone radius
C	heat capacity
c	specific heat
Cf	correction factor
E	measured voltage across known load
$F_{( )}$	view factor
f	frequency
h	dimension
K	thermal conductivity; calibration constant
k	Boltzmann constant; thermal diffusivity constant
l	length
ℓ	heater lead resistance
M	mass
r and R	resistances
RC	resistance–heat capacity time constant
r	radius
T	temperature
t	time
t	thickness
v	output electromotive force
W	thermal energy (watts)
α	absorptivity
ϵ	emissivity
ρ	material density
σ	Stefan–Boltzmann constant

Subscripts

ap	aperture
cav	cavity
coat	coating
hs	heatsink
in	input
l	loss
m	metallic
muf	muffler
o	output
r	radiative
VL	view-limiting tube

References

1. Kendall, J. M., *The JPL Standard Total Radiation Absolute Radiometer,* Technical Report 32-1263. Jet Propulsion Laboratory, Pasadena, Calif., May 15, 1968.
2. Sparrow, E. C., and Jonsson, V. K., "Radiant Emission Characteristics of Diffuse Cavities," *J. Opt. Soc. Am.,* Vol. 53, pp. 816–821, July 1963.
3. *Eppley–Parsons Optical Black Lacquer,* Advertising Brochure. Eppley Laboratory, Inc., Newport, R. I.
4. Blevins, W. R., and Brown, W. J., "Black Coatings for Absolute Radiometers," *Metrologia,* No. 2, pp. 139–143, Aug. 1966.
5. Eckert, E. R., and Drake, R. M., *Heat and Mass Transfer,* Second Edition, p. 398. McGraw-Hill Book Co., Inc., New York, 1959.
6. Carslaw, H. S., and Jaeger, J. C., *Conduction of Heat in Solids,* Second Edition, p. 97. The Oxford Press, Oxford, England, 1959.